REGULATION OF PROTEIN SYNTHESIS BY INTERFERON β IN ATAXIA-TELANGIECTASIA CELLS

by

Chanda Siddoo-Atwal

B.Sc., University College London, 1989

THESIS SUBMITTED IN PARTIAL FULFILMENT OF

THE REQUIREMENTS FOR THE DEGREE OF

DOCTOR OF PHILOSOPHY

in the School of Kinesiology

Simon Fraser University

April 1996

APPROVAL

NAME: Chanda Siddoo-Atwal

DEGREE: Doctor of Philosophy

TITLE OF THESIS: REGULATION OF PROTEIN SYNTHESIS BY INTERFERON β IN ATAXIA-TELANGIECTASIA CELLS

EXAMINING COMMITTEE:

Chair: Dr. John Dickinson

Dr. Miriam Rosin
Senior Supervisor
Professor, School of Kinesiology

Dr. Allan Davison
Professor, School of Kinesiology

Dr. Arthur Haas
Professor, Department of Biochemistry
Medical College of Wisconsin

Dr. Margo Moore
Assistant Professor, Biological Sciences

Dr. Anne Autor
Internal Examiner
Pathology and Laboratory Medicine
University of British Columbia

Dr. Malcolm Paterson
External Examiner
Director Molecular Oncology Program
Cross Cancer Institute

Date Approved: April 15/96

PARTIAL COPYRIGHT LICENSE

I hereby grant to Simon Fraser University the right to lend my thesis, project or extended essay (the title of which is shown below) to users of the Simon Fraser University Library, and to make partial or single copies only for such users or in response to a request from the library of any other university, or other educational institution, on its own behalf or for one of its users. I further agree that permission for multiple copying of this work for scholarly purposes may be granted by me or the Dean of Graduate Studies. It is understood that copying or publication of this work for financial gain shall not be allowed without my written permission.

Title of Thesis/Project/Extended Essay

REGULATION OF PROTEIN SYNTHESIS BY INTERFERON β IN ATAXIA-TELANGIECTASIA CELLS

Author:
(signature)

CHANDA SIDDOO-ATWAL
(name)

April 15, 1996
(date)

ABSTRACT

Ataxia-telangiectasia (AT) is an autosomal recessive genetic disorder which is characterized by loss of coordination and telangiectases, hypersensitivity to ionizing radiation, progressive neuronal degeneration, immunodeficiency and increased cancer risk. Recently, the ATM (mutated in AT) gene has been cloned and been shown to bear significant homology to phosphatidylinositol 3-kinases (PI3Ks) suggesting that its product may function in signal transduction. It has been reported that the NF-κB transcription factor is constitutively activated in AT cells, possibly as a result of the ATM gene product. NF-κB is an inducer of the interferon ß gene. Since interferon ß produces a wide range of biological effects including slowing of cell proliferation, virus inhibition, immunomodulation and alterations in differentiation, a dysfunction of interferon ß regulation could have serious consequences for the cell. Therefore, the hypotheses investigated in this thesis were that the levels of interferon ß-inducible proteins are elevated in AT cells as a result of constitutive activation of the interferon ß induction pathway; altered ubiquitin cross-reactive protein (UCRP) kinetics may be linked to cell cycle differences that exist between AT and normal cells; and dysregulation of the interferon ß induction pathway may be related to cancer.

Using immunohistochemistry, elevated levels of UCRP were observed in two distinct fibroblast cell lines derived from patients with AT when compared to controls. Immunofluorescence studies suggested that differences in UCRP localization may normally occur between dividing and stationary cells, while UCRP levels are constitutively elevated in dividing and stationary AT cells.

Immunoblotting experiments showed elevation of free UCRP, not conjugated UCRP, in AT cells. A low molecular weight protein, LMP2, which is a proteasome

subunit, was also found to be elevated in AT cells. However, the induction by interferon ß of free UCRP, UCRP conjugates and of LMP2 was the same in normal and AT cells, suggesting that AT cells possess a defect in the regulation of interferon ß levels. Culturing three successive passages of an AT cell strain in the presence of different concentrations of neutralizing antibodies against interferon ß caused partial and complete reduction, respectively, of free UCRP and LMP2 immunoreactive proteins to normal levels. These results indicate that there is a constitutive activation of the interferon ß induction pathway in AT cells, which causes the secondary activation of interferon ß-inducible proteins.

Since AT cells are susceptible to cancer, a mechanism involving constitutive activation of the interferon ß induction pathway may also be responsible for upregulation of interferon ß-inducible proteins in cancer cells. A preliminary study of UCRP levels in human lung and bladder cancer tissue showed that these tissues had elevated UCRP levels. Thus, this mechanism could represent an early mutational event in carcinogenesis that dysregulates the activation pathway for the interferon ß gene.

ACKNOWLEDGEMENTS

I would like to acknowledge my eternal debt to Dr. Margo Moore, who encouraged me to continue with my Ph.D. at a time I thought it was no longer possible, and to Dr. Arthur Haas, who has been my guiding light and without whose help this thesis would not have been possible. I would also like to acknowledge my gratitude to my father and angel mother, who have stood by me through all my endeavours and to my many friends, who helped to lighten my darkest hours... and to Dr. Glen Tibbits, who was also one of my lights...and to the people at IMC, who were so patient with me...and to the ladies in the Kinesiology office, who brightened my days with their smiles. My special thanks to all of you!

I would like to thank Dr. Miriam Rosin, who was my major advisor and provided the necessary facilities for my research in her lab, Dr. Wade Parkhouse, who very kindly provided some of the equipment for my experiments, and Dr. Allan Davison, who was a supportive member of my committee. I would also like to thank all the other people who were so generous in sharing their technical expertise with me, especially Dr. Silia Chadan.

I would like to commend each of my committee members on the superb job they did in editing the thesis.

Finally, I would like to dedicate this thesis to all those children with ataxia-telangiectasia in the hope that this work will benefit them in some way.

TABLE OF CONTENTS

LIST OF FIGURES

Introduction

Elevation of Interferon ß-Inducible Proteins in Ataxia-telangiectasia Cells

Immunolocalization of UCRP in Ataxia-telangiectasia Cells

A Preliminary Study of UCRP Levels in Human Lung and Bladder Cancers

Conclusion

LIST OF TABLES

Introduction

A Preliminary Study of UCRP Levels in Human Lung and Bladder Cancers

LIST OF ABBREVIATIONS

AT	ataxia-telangiectasia
ATM	AT mutated
PI3K/PI 3-kinase	phosphatidylinositol 3-kinase
DNA-PK	DNA-dependent protein kinase
DSBs	double-stranded breaks
UCRP	ubiquitin cross-reactive protein
LMP2	low molecular weight protein
IFN ß	interferon ß
IL-6	interleukin-6 (interferon ß)
CDK	cyclin-dependent kinase
CDI	cyclin-dependent kinase inhibitor
MHC	major histocompatibility complex
ISGF	interferon-stimulated gene factor
ISRE	interferon-stimulated response element
ISG	interferon-stimulated gene
IRF	interferon regulatory factor
PRD	positive regulatory domain
UV	ultraviolet
Rb	retinoblastoma
TGF	transforming growth factor
PCNA	proliferating cell nuclear antigen

THESIS FORMAT

As a non-traditional thesis, the organization of this thesis requires some introduction. This thesis has six main sections: general introduction, experimental approach, three papers written for publication, and general conclusion.

The general introduction provides the background for all of the research presented in the thesis.

The experimental approach outlines the hypotheses that were tested and details the development of the methodology that was followed in the ensuing papers.

The first paper describes the novel observation that the levels of two interferon ß-inducible proteins are elevated in ataxia-telangiectasia cells and that their elevation can be inhibited by treating the cells with neutralizing antibodies against interferon ß. This paper also explores the possible events that may lead to UCRP elevation in AT cells.

The second paper investigates differences in UCRP immunolocalization between normal and AT fibroblasts at different stages of cell division and discusses the possibility that the differences observed may play a role in determining cell cycle events.

The third paper is a feasability study which examines UCRP levels in various human tumour tissues and attempts to put the findings in context with UCRP elevation in AT cells and with the cancer proneness associated with this disease. Further work with proper control tissues is still to be carried out.

The general conclusion attempts to unify the findings of this thesis, put them in context with the existing literature, and to propose new directions of research suggested by this work.

INTRODUCTION

1.1 Ataxia-telangiectasia Syndrome

The first clinical report of ataxia-telangiectasia was published by Syllaba and Henner in 1926, followed by a second clinical description by Denise Louis-Bar in 1941. The ataxia-telangiectasia (AT) syndrome was first named after two of its major characteristics in 1952 by Boder and Sedgwick, who identified a number of patients with similar symptoms [1]. Genetic studies soon revealed that the multi-faceted AT syndrome is inherited in an autosomal recessive fashion. The worldwide incidence of AT varies from 1 in 40,000 to 1 in 100,000 and patients usually die during the second or early third decade of life [2].

Clinically, AT patients are characterized by loss of coordination and telangiectases, hypersensitivity to ionizing radiation, progressive neuronal degeneration, immunodeficiency, and cancer proneness [3,4]. Dilated blood vessels (telangiectases) occur in the conjunctivae of the eye, the facial skin, and sometimes in other sunlight-exposed areas of the body. Immunological deficiencies include absence or underdevelopment of the thymus and severe deficiencies in the humoral and cellular immune responses that can cause recurrent sinopulmonary infections. The cancer proneness of AT homozygotes is manifested as a predisposition to lymphoreticular malignancies. On the other hand, AT heterozygotes have a 4.0 fold increase in relative risk for breast cancer [4].

The cellular features of AT lymphocytes, lymphoblasts, or fibroblasts include hypersensitivity to ionizing radiation and radiomimetic drugs and elevated spontaneous chromosomal instability [3,4,5].

One of the most common characteristics of cell lines derived from AT patients is that they do not undergo the inhibition of DNA synthesis that is typical of normal

cells following ionizing radiation treatment [6,7]. Following ionizing radiation treatment, normal cultured cells block in either G1-S or G2-M, depending on which phase of the cycle they are in, to repair the DNA damage caused by the X-rays. Similarly cells block in S phase in response to X-rays [1]. In AT cells, however, flow cytometric studies have consistently revealed that AT cells do not undergo an X-ray induced cell cycle arrest in G1 and G2 phases, but undergo a subsequent delay in G2/M [8,9]. Delayed cell cycle progression in AT cells treated with X-rays is also observed [1].

Initially, the AT locus was localized to the q22-23 region of chromosome 11 by linkage analysis [10]. Recently, the ATM gene, which is mutated in ataxia-telangiectasia was identified by positional cloning on chromosome 11 [2,11]. Four complementation groups, A,C,D, and E have been identified in AT by characterizing heterokaryons and the ATM gene was found to be mutated in AT patients from all complementation groups. Thus, mutations in this gene are probably the sole cause of this disease.

The pleiotropic nature of AT mutations may be explained by the "mosaic" structure of the ATM protein which has domains similar to other known proteins. The COOH-terminal of the ATM gene product is highly similar to the catalytic subunit of several yeast and mammalian phosphatidylinositol 3-kinases (PI3Ks) which are involved in mitogenic signal transduction, meiotic recombination, and cell cycle control. Another region closer to the N-terminus of the protein bears close homology to the yeast rad3 and mec1 DNA repair/cell-cycle checkpoint genes [12].

PI3K is a heterodimer composed of a 110 kDa subunit and an 85 kDa subunit. The catalytic domain resides in the 100 kDa subunit, while the 85 kDa subunit may have a regulatory role. Recent studies have indicated that the 110 kDa subunit may display both lipid kinase and serine/threonine protein kinase activity. PI3K has been

shown to phosphorylate phosphatidylinositol at the D-3 position of the inositol ring to produce phosphatidylinositol 3-phosphate. However, the resulting 3-phosphorylated lipids are not hydrolyzed and are not components of the phosphoinositide cascade suggesting phosphatidylinositol 3-phosphate itself may act as a second messenger that mediates the effects of activated PI3K. Inducers of PI3K activity include certain growth factors such as platelet-derived growth factor (PDGF), colony stimulating factor 1 (CSF-1), insulin-like growth factor 1 (IGF-1), epidermal growth factor (EGF), nerve growth factor (NGF), and stem cell growth factor and elevated PI3K activity has been found to be associated with cells transformed by polyoma middle T, v-src, v-fms, and v-abl [55].

DNA-dependent protein kinase (DNA-PK), a serine/threonine kinase, is a member of the phosphatidylinositol 3-kinase (PI3K) family [39] and is also related to the ATM gene product [40]. DNA-PK shows no detectible activity towards lipids, but it is most similar to PI kinases that are involved in cell cycle control, DNA repair and DNA damage responses [40]. This particular protein kinase is activated by double-stranded breaks (DSBs) or other discontinuities in the DNA double helix. In fact, cells that are defective in components of the DNA-PK recognition pathway are hypersensitive to killing by X-rays, as they are unable to repair DSBs effectively. In addition, DNA-PK phosphorylates several transcription factors including p53, Sp1, Fos, Jun, and Myc and is a potent inhibitor of transcription by RNA polymerase I suggesting that it is a modulator of checkpoint mechanisms activated by DNA damage [41].

Following exposure to DNA damaging agents, an elaborate signal transduction pathway involving DNA-PK is initiated in mammalian cells. The activation of plasma membrane receptor tyrosine kinases results in the activation of c-ras (RAS-GTP), which, in turn, leads to the activation of a serine/threonine kinase cascade that

Figure 1. Signal Transduction Following DNA Damage in Mammalian Cells[1]

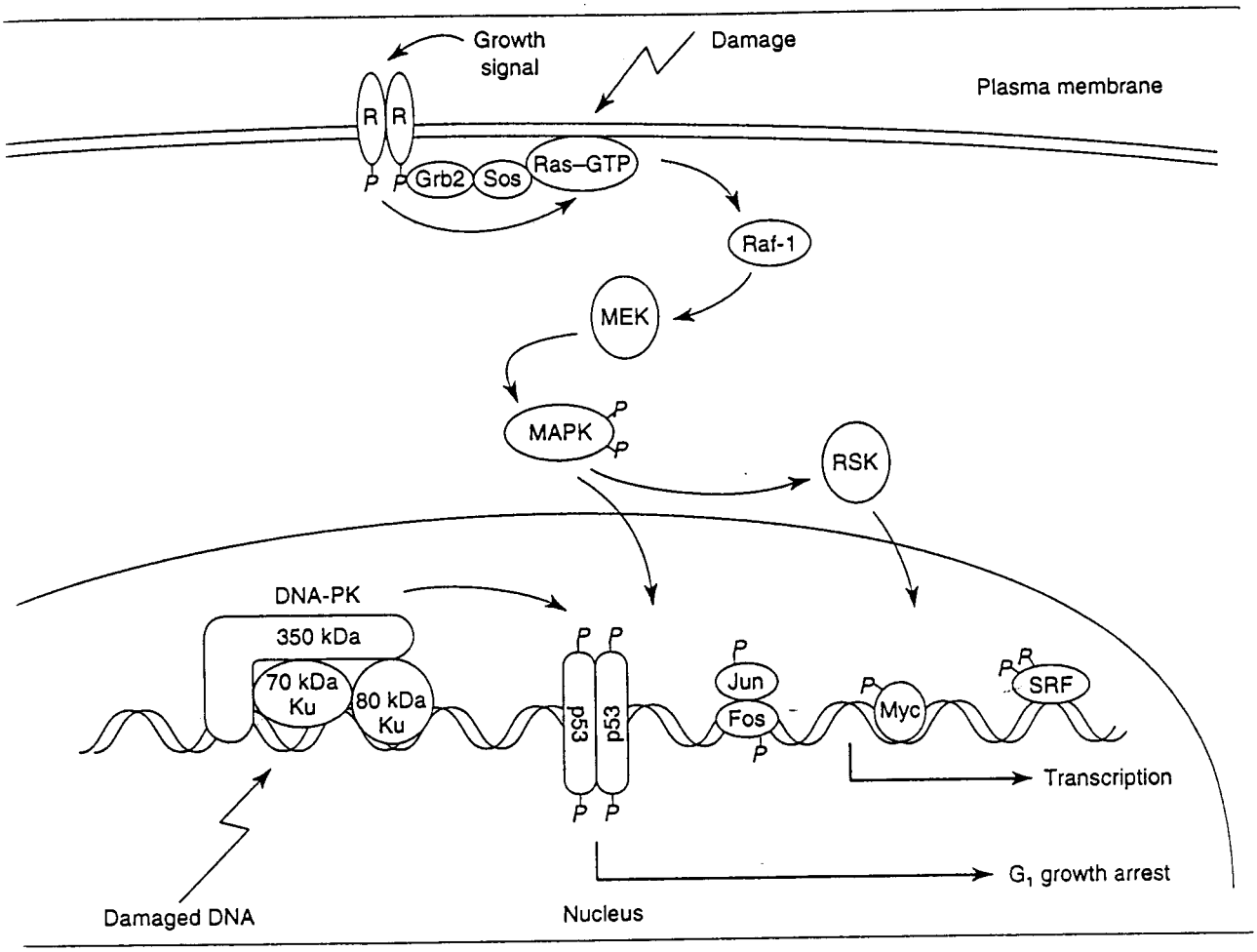

[1] All data are from reference [41].

includes mitogen-activated kinase (MAPK) and MAPK-activated protein kinases. Targets of the MAP kinases include immediate-early transcription factors, such as Jun, Fos, Myc, and SRF. At the same time, DNA damage activates DNA-PK to target these same transcription factors and p53, which is stabilized through a post-translational mechanism and activates the G1 checkpoint growth-arrest mechanism (See Figure 1) [41]. In addition, stress-activated (SAP) protein kinases, that are related to the MAP kinase family, are activated by tumour necrosis factor, UV light, and Ha-ras to phosphorylate the activation domain of c-jun [42]. Therefore, even though the exact biochemical function of ATM remains unknown, it seems possible that the ATM defect may be in some aspect of this pathway, the dysregulation of which ultimately manifests itself as the high cancer incidence observed in AT patients.

Growing evidence suggests that the ATM protein is involved in the signal transduction of a DNA damage surveillance network that also includes initiation of apoptosis in response to low doses of ionizing radiation [56]. A high frequency of spontaneous apoptosis has been observed in Purkinje and granule cells in AT patients and inappropriate apoptosis has been reported in AT cells in response to X-rays [56,57,58]. Together, these observations support a model in which a DNA damage response pathway involving apoptosis is deregulated in AT cells.

1.2 Cancer and the Cell Cycle

Cancer is a disease of uncontrolled cell division. Diminished growth control causes malignant cancer cells to invade local tissues and, eventually, to spread to other parts of the body. This colonization can interfere with the body's vital functions and prove to be incompatible with life. Our understanding of cancer, therefore, is limited by our present understanding of cell growth and division.

Cancer cells contain genetic damage, which appears to be the cause of carcinogenesis. Two types of genes have been implicated in the development of cancer. Various proto-oncogene products are known to stimulate cell cycle progression, whereas various tumour suppressor gene products inhibit cell cycle progression. A great deal of experimental evidence has accumulated to show that activated or altered proto-oncogene expression and loss or inactivation of tumour suppressor gene expression can contribute significantly to the tumour cell phenotype [13]. Proto-oncogenes can be converted to oncogenes via point mutations, small insertions or deletions, and juxtaposition to other chromosome sequences resulting in higher transcription rates. On the other hand, in general, both copies of a tumour suppressor gene must be inactivated by mutation or deleted via loss of the entire gene, a region of the chromosome, or the entire chromosome in order to produce oncogenicity, since their action is growth inhibitory [13].

In the last decade, numerous connections between oncogenesis and the regulatory components of the cell cycle have been discovered. Most of the components implicated in cancer through mutation or overexpression, or through their absence in tumours or transformed cells, have been found to act at specific points upon the cell cycle (See Figure 2). Briefly, the cell cycle is composed of chromosome duplication followed by segregation of the genomes into two daughter nuclei; subsequent cytokinesis gives rise to two independent new cells. Various phases of the cell cycle have been delineated, G1, S, G2, M, and G0. G0 represents the state of non-cycling cells. G1 and G2 are known as the "gap" phases that occur before S and M phases, respectively. Each "gap" is characterized by preparation for the phase that directly follows it. S is the synthetic phase of the cycle during which DNA synthesis and doubling of the genome occurs. M is the mitotic phase during which the duplicated chromosomes segregate. If the right conditions for S and M

Figure 2. Cell Cycle Regulators Implicated in Cancer[1]

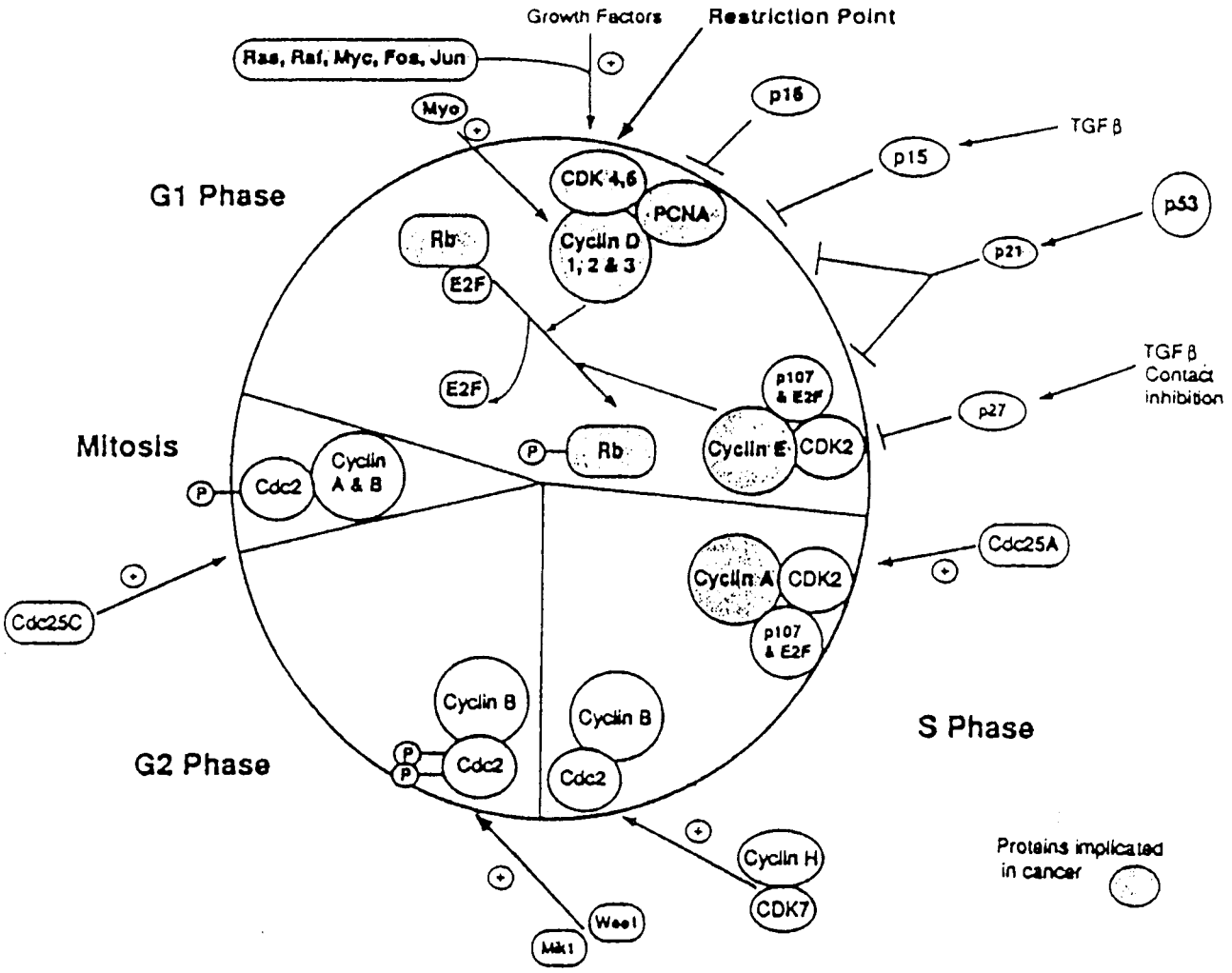

[1] All data are from reference [16].

phases do not prevail, for example, in the case of DNA damage or nutrient unavailability, then, in most cases, the cell may block the cycle in G1 or G2. Thus, the G1-S transition and the G2-M transition can serve as important cell cycle checkpoints to ensure viability of the cell under adverse circumstances [14,15].

A group of proteins known as cyclins and cyclin-dependent kinase proteins (CDKs) regulate the cell cycle and its transitions. The cyclins can be divided into G1 cyclins (cyclins C, D1, D2, D3, E and F), S-phase cyclins (cyclin A) and mitotic cyclins (cyclins B1 and B2) [15]. At least one class of cyclin, cyclin H, has been found to be present throughout all phases of the cell cycle and the specific cell cycle role of another cyclin, cyclin G, is presently unknown [16].

Generally, according to the phase of the cell cycle, the corresponding cyclins associate with stage-specific CDKs thereby activating them and driving the cell cycle on (See Table 1). Once each cyclin has activated its CDK, its level generally declines rapidly via the ubiquitin conjugation system or some other degradative mechanism [18,19]. For example, cyclins A and B are targetted for degradation via conjugation with ubiquitin. Both contain a 9 amino acid sequence in their carboxyl terminal, the "destruction box", that is thought to be recognized by some component of the ubiquitin conjugating system [17,18]. In contrast, human G1 cyclins (C, D, and E) have been found to contain a PEST sequence in their carboxy terminus that is implicated in rapid protein degradation by an unidentified mechanism [19]. The Saccharomyces cerevisiae G1 cyclin, CLN2 (the yeast homologue of the human D cyclins) contains a sequence which bears weak homology to the "destruction box" of cyclins A and B [18], which implies that G1 cyclin levels in humans may also be regulated via ubiquitin conjugation.

Recently, a family of small cyclin-dependent kinase inhibitor proteins (CDIs) that bind to and inactivate the CDKs has also been isolated [16]. It is therefore not

Table 1. Cyclin-CDK Complexes[1]				
Cyclin	Cell Cycle Role	Associated CDK	Stability	Degradation
A	S plus G2→M	Cdc2 and CDK2	Unstable in mitosis	Ubiquitin
B1	G2→M	Cdc2	Unstable in mitosis	Ubiquitin
B2	G2→M		Unstable in mitosis	Ubiquitin
C-type	?	CDK X?	ND	PEST
D1	G1	CDK4	Rapid turnover	PEST
D2	G1	CDK4	Rapid turnover	PEST
D3	G1	CDK4	Rapid turnover	PEST
All D-types				
E	G1 plus G1→S	CDK2	Rapid turnover	PEST
F			ND	
G			ND	
H	All phases	CDK7	ND	ND
ND, not determined				

[1] All data are from reference [16].

surprising that the persistent expression of certain cyclins has led to their identification as proto-oncogene products and that individual inhibitor proteins have often been found to be absent from transformed cells thereby resembling inactivated tumour suppressors [16].

1.3 Ubiquitin Conjugation and Protein Degradation

The ATP-dependent ubiquitin conjugation system for intracellular protein degradation is common to all eukaryotic cells. Once covalent attachment of ubiquitin tags a protein, it is recognized and degraded by a non-lysosomal, cytosolic protease complex, known as a proteasome [20,21].

Several steps are involved in the conjugation of ubiquitin, which is an 8.6 kDa protein, to its target proteins (See Figure 3). Firstly, ubiquitin is activated to form ubiquitin-adenylate. Secondly, ubiquitin complexes with the activating enzyme E1 and is transferred to a site where it forms a thiol ester between its terminal carboxyl and a sulphydryl group on the enzyme. Thirdly, the ubiquitin is transferred to the thiol group of E2, a ubiquitin-conjugating enzyme. Lastly, ubiquitin is ligated to the target protein by forming a peptide bond between its terminal carboxyl group and an amino group of a lysine on the target protein. This process may require additional "ligation" enzymes called E3s. Multi-ubiquitin chains with up to 20 units ligated to the lysine (Lys-48) of the target protein-bound ubiquitin molecule may be formed. Furthermore, ubiquitin may also be conjugated to more than one lysine residue on a given target protein. Support for the hypothesis that formation of multi-ubiquitin chains rather than single ubiquitination is required for degradation comes from a study which showed that a mutant ubiquitin molecule with a cysteine substituted for lysine at position 48 did not form multi-ubiquitin chains and did not tag its target protein for proteolysis [22].

Figure 3. The Ubiquitin Conjugation Pathway[1]

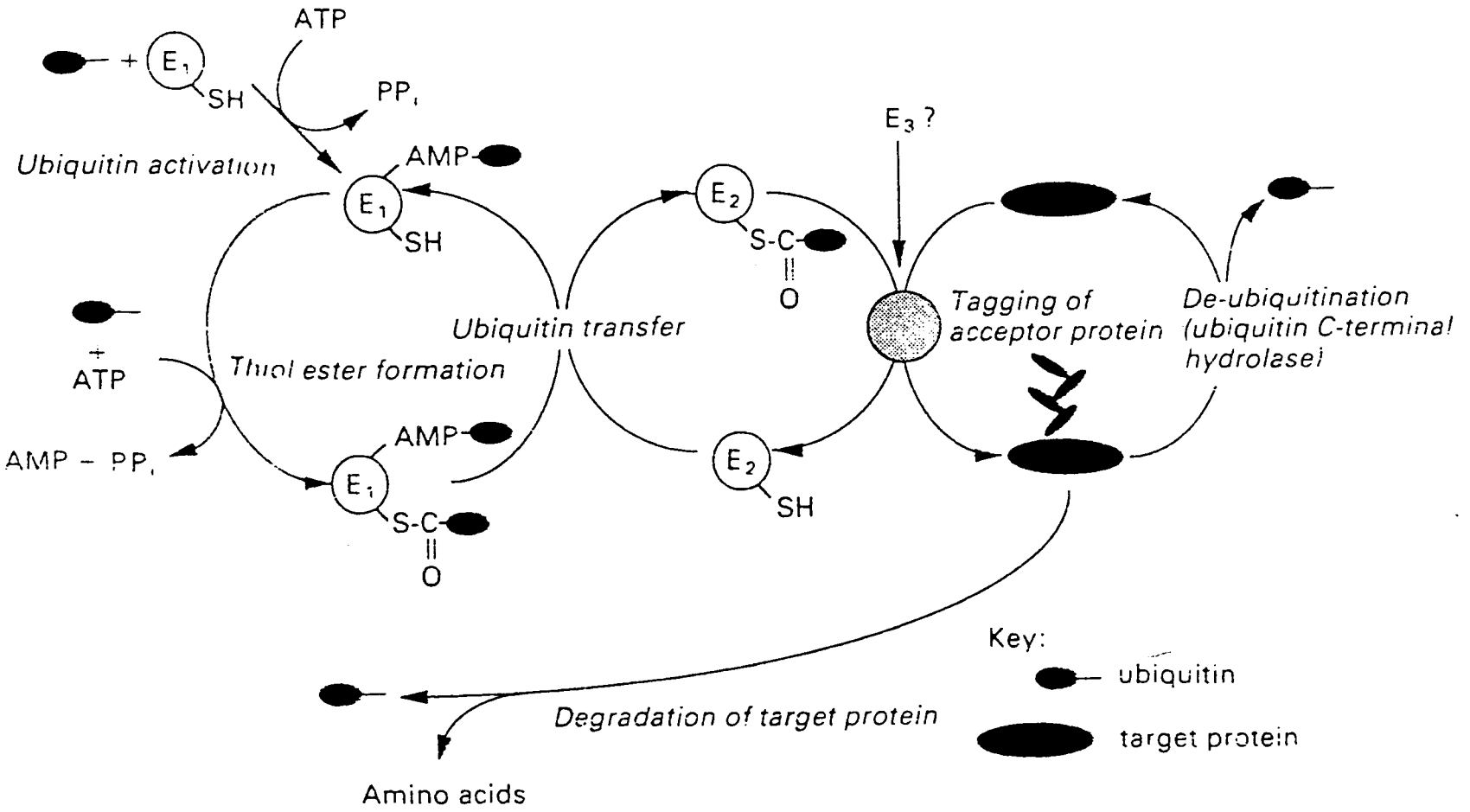

[1] All data are from reference [22].

Besides degrading ubiquitinylated proteins, proteasomes are also involved in degrading non-assembled protein subunits, regulatory proteins, and metabolically regulated enzymes [23]. Two types of proteasomes, 20S and 26S, have been distinguished according to their sedimentation coefficients. 20S proteasomes are composed of a set of small subunits belonging to the α- or ß-subunit family (See Table 2), while 26S proteasomes are composed of a central 20S proteasome and two terminal subsets of other multiple subunits attached to the central core in opposite orientations (See Table 3) [24]. Interestingly, in response to certain extracellular signals such as interferon γ and to a lesser degree interferon ß, some ß-type subunits appear to be replaced by different but homologous ß-subunits thereby altering the specificity of proteasomes. For example, interferon γ was found to induce the synthesis of the MHC-encoded proteasome subunits LMP2 and LMP7 and result in the almost complete loss of proteasome subunits X and Y in various human cells. The proteasomes synthesized following interferon γ treatment showed increased trypsin- and chymotrypsin-like activity, while peptidylglutamyl-peptide-hydrolyzing activity was depressed. However, the ATP-, ubiquitin-dependent activity of the newly assembled proteasomes was not affected. Thus, it appears that functional diversity can be acquired through altering proteasome subunit assembly following cytokine treatment [25].

The ubiquitin-proteasomal pathway is involved in the programmed destruction of several regulatory proteins including cyclins, p53, c-mos, c-myc, c-fos and c-jun that are closely connected to cell cycle progression [26,27]. The ubiquitin-proteasome system is also responsible for activation of the NF-κB transcription factor by converting the p105 precursor protein into its p50 and p65 subunits and by degrading the IκB inhibitory protein [28]. In addition, it is involved in the removal of abnormal proteins in the cell [24].

Table 2. 20S Proteasome Subunits[1]	
Human	MW
α-Type Subunit	
HC2 (PROS-30)	29555
HC3	25898
HC8	28433
HC9	29483
PROS-27(IOTA)	27374
ZETA	26425
XAPC7	27900
ß-Subunit	
HC5	26489
HC7-1	22836
HC10-11	22931
HN3	29192
X (MB1)	22897
Y (DELT)	25315
Z	29965
LMP7-E1	29769
LMP7-E2	30354
LMP2	23245
MECL1	28936

Table 3. 26S Proteasome Regulatory Subunits[1]	
Human	MW
ATPase subunit	
S4	49239
MSS1 (S7)	48633
TBP-1	45164
TBP-7	51550
p45	45770
Non-ATPase subunit	
p11 2(S1)	105864
p97 (S1)	
p58	60623
p31	30004
p28	
S5	
S12	

[1] All data are from reference [24].

There is much evidence to suggest that the ubiquitin-proteasome pathway plays an essential role in cell growth and division. Disruption of yeast genes encoding proteasomal subunits causes the complete cessation of cell growth followed by cell death indicating the essential role of proteasomes in the eukaryotic cell cycle [29]. Proteasomes are highly expressed in rapidly growing embryonic tissues of rats, chicks, Xenopus, and Drosophila. Moreover, proteasomal expression has been found to be high in all cancer cells examined including human hepatoma, leukemia, and primary kidney cancer cell lines [29]. Various ubiquitin species are also elevated in leukemic and renal cancer cells [29]. In addition, high concentrations of proteasomes have been found to be associated with spindle microtubules in dividing cells. In contrast, treatment of leukemic cells with compounds such as phorbol esters, dimethylsulfoxide, retinoic acid or butyric acid that induce differentiation into monocytes, granulocytes, and erythrocytes results in the down-regulation of proteasomal subunits and ubiquitin [29].

There is evidence to suggest that changes in ubiquitin conjugation kinetics, at specific points in the cell cycle, can result in altered cell cycle regulation. For example, a yeast cell cycle mutant with a post-irradiation defect similar to AT has been well characterized. These mutants of S. cerevisiae (RAD6) are extremely sensitive to DNA damage caused by ultraviolet light, X-rays and chemical mutagens, as they are totally deficient in repairing the mutations caused by these agents. The RAD6 gene encodes a ubiquitin-conjugating enzyme of the E2 family [30]. A homologous gene, the yeast CDC34 gene, encodes a related ubiquitin-conjugating E2 isozyme that is required for the transition of cells from G1 to S phase in the cell cycle [31]. The RAD9 mutant of S. cerevisiae is also highly sensitive to radiation and is characterized by the absence of a radiation-induced G2 delay [32]; it may encode a related protein that is involved in ubiquitin conjugation. Further support comes from

studies using yeast to express a mutant ubiquitin molecule that irreversibly conjugates to protein thereby gradually depleting ubiquitin stores. The cells expressing this protein display characteristics consistent with ubiquitin deficiency or a mutant deficient in ubiquitin conjugation. They have slow growth and sensitivity to various forms of environmental stress and to ultraviolet light [33].

1.4 Ubiquitin Cross-Reactive Protein (UCRP)

Originally, ubiquitin cross-reactive protein (UCRP) was identified as a 15 kDa protein that was released by interferon ß-induced human lymphocytes and monocytes into the surrounding medium [34]. Subsequently, it was found to consist of two domains, both of which bear significant homology to ubiquitin. The amino-terminal domain of UCRP displays 40% homology and the carboxyl-terminal domain shows 53% homology to ubiquitin at the amino acid level. Immunological cross-reactivity was demonstrated by cross-reaction of UCRP with affinity-purified antibodies against SDS-denatured ubiquitin using immunoblot analysis and solution phase radioimmunoassay [35]. Homology between residues that determine the secondary structure of ubiquitin indicates that both proteins may share a common folding motif. The fact that UCRP has the same hexapeptide sequence required for activation of the mature peptide during isopeptide bond formation and recognition for processing in its COOH-terminal as ubiquitin, suggests that the two proteins undergo similar enzymatic transformations. Like ubiquitin, UCRP is conjugated to other proteins and it has been proposed that such adduct formation may mediate some of the diverse biological effects of interferon [36].

UCRP is one of the earliest genes induced following interferon α or ß treatment and is observed in all cell types sensitive to these cytokines [36]. Low levels of interferons are present in most human tissues, however biological stimuli including

infection by various viruses, bacteria, mycoplasma and protozoa, and exposure to certain cytokines and growth factors such as interleukin-1, interleukin-2, tumour necrosis factor, and colony-stimulating factor-1 enhance their biosynthesis.

NF-κB, which is activated by a variety of DNA damaging agents including UV light and X-rays via a complex pathway (See Table 4) [43], is an important transcriptional activator of the interferon ß gene, but, apparently, only in response to virus infection (See p.42) [44]. NF-κB helps to induce an antiviral status involving growth arrest in interferon-induced cells. However, NF-κB is not sufficient on its own to activate the interferon ß gene promoter. The promoter region of the human interferon ß gene is made up of four positive regulatory domains (PRD), PRDI-PRDIV, each of which binds a different transcription factor. Members of the interferon regulatory factor (IRF) family of transcription factors bind to both PRDI and PRDIII; the NF-κB heterodimers, p50 and p65, bind to PRDII; the ATF-2 homodimer or the ATF-2-c-jun heterodimer binds to PRDIV; and HMGI(Y) binds to the AT-rich region within PRDII and to the two AT-rich sequences flanking the ATF binding site in PRDIV. Induction of the interferon ß gene requires coordinate activation of each of the PRDs [45].

Once they are induced, interferons usually act in a paracrine fashion. Interferons α and ß compete for the same cell-surface receptors on target cells and interferon α is known to activate interferon-stimulated gene factor-3 (ISGF-3) as a result of the signal that is generated by the occupied receptor. In turn, ISGF-3 mediates the transcriptional activation of interferon-inducible genes by binding to the interferon-stimulated response element (ISRE) in their 5'-flanking regions. This results in the rapid activation of a large set of genes (including UCRP) that are involved in mediating the antiproliferative and antiviral effects of the type I interferons (interferons α and ß) (See Figure 4) [36,37]. Interferon induction also

stimulates the conjugation of UCRP to various proteins [36]. Thus far, UCRP has been found to conjugate to proteins that bind to cytoskeletal elements including several types of intermediate filaments such as keratin and vimentin [38]. In addition, interferon ß manifests some of its antigrowth effects by reducing the mRNA expression of Myc, Ras, cyclin A and cyclin Ds, factors that control entry into S phase of the cell cycle [46]. Interestingly, an unidentified protein, ATDC, has been isolated on the basis of its ability to complement the ionizing radiation sensitivity of AT group D fibroblasts and the ATDC protein interacts with vimentin [59].

1.5 Summary

The study of ataxia-telangiectasia provides a unique opportunity to examine a "proto-cancer" cell and to identify any biochemical changes that may be related, in part, to its predisposition to cancerous transformation. Even though no singular event is likely to be responsible for carcinogenesis, the AT mutation results in drastic changes to the cell cycle. AT cells closely resemble yeast cell cycle mutants that have mutations in ubiquitin conjugation. Furthermore, ubiquitin has been found to play an important role in the cell cycle. Interestingly, however, ubiquitin cross-reactive protein (UCRP), not ubiquitin, has been found to be dysregulated in AT cells. Therefore, like its relative ubiquitin, this interferon ß-inducible protein could be involved in cell cycle regulation.

Table 4. Inducers of NF-*k*B[1]	
Class	Inducing condition
Bacterial products	Lipopolysaccharide Exotoxin B Toxic shock syndrome toxin 1 Muramyl peptides
Viruses	Human immunodeficiency virus type 1 (HIV-I) Human T cell leukemia virus type I (HTLV-1) Hepatitis B virus (HBV) Herpes simplex virus type 1 (HSV-1) Human herpes virus 6 Newcastle disease virus Sendai virus Epstein-Barr virus (EBV) Adenovirus
Viral products	Double-stranded RNA Tax (from HTLV-1) HBx (from HBV) MHBs (from HBV) Epstein-Barr nuclear antigen 2 (EBNA-2, from EBV) Latent membrane protein (LMP, from EBV)
Eukaryotic parasite	*Theileria parva*
Inflammatory cytokines	Tumor necrosis factor α Lymphotoxin Interleukin-1 Interleukin-2 Leukotriene B4 Lymphocyte inhibitory factor
T cell mitogens	Antigen Lectins (PHA, ConA) Calcium ionophores Anti-CD3 Anti-CD2 Anti-CD28
ß cell mitogen	anti-surface lgM
Fibroblast mitogen	Serum
Protein synthesis inhibitors	Cycloheximide Anisomycin
Physical stress	UV light γ radiation
Oxidative stress	Hydrogen peroxide Butyl peroxide
Drugs	Okadaic acid Phorbol esters

[1] All data are from reference [43].

Figure 4. Interferon β Induction of Proteins

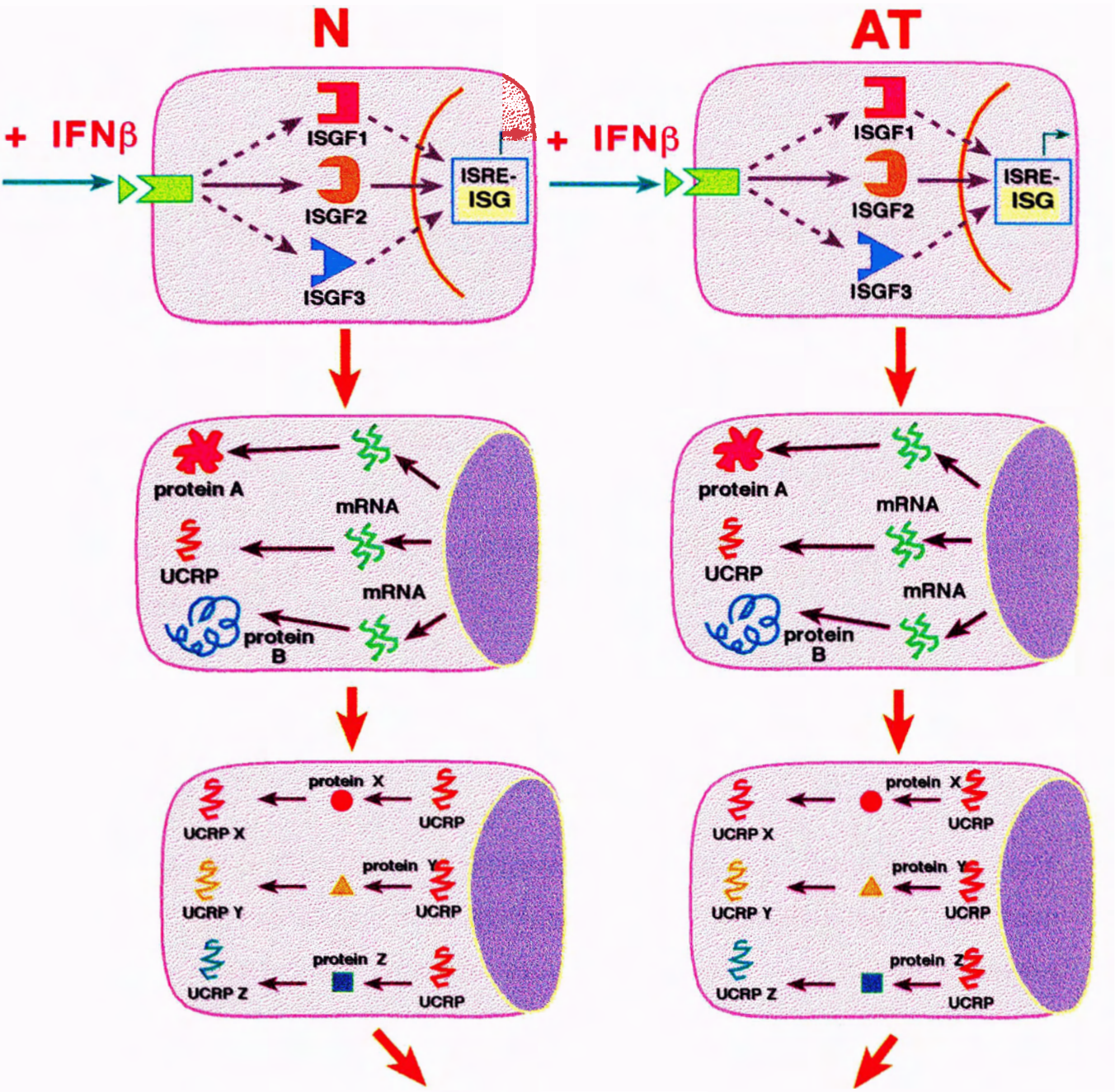

a) virus inhibition
b) alterations in differentiation
c) immunomodulation
d) cell cycle effects
   - inhibition of c-myc, ras expression
   - inhibition of cyclin A, D_1, D_2 expression
   - complementation of p53 action
   - UCRP-(cytoskeletal) protein conjugates?

EXPERIMENTAL APPROACH

The central hypotheses addressed in this thesis are outlined below.

1. The levels of interferon ß-inducible proteins are elevated in certain AT cells as a result of dysregulation of the interferon ß induction pathway.

2. The elevation of UCRP levels resulting from the dysregulation of the interferon ß induction pathway in AT cells may be related to the cell cycle differences that exist between AT and normal cells.

3. Dysregulation of the interferon ß induction pathway may be an early step in carcinogenesis.

The background for the experimental techniques employed in this thesis is presented below.

Cell Culture - The human fibroblast cell strains for these studies were obtained from a cell repository, thus limiting selection. Relatively old AT cell lines with a reasonable growth potential and doubling efficiency close to that of normal cells, and normal cell lines with a normal karyotype (since not all the normal cell lines at the repository had normal karyotypes), were chosen. These cell lines were matched as closely as possible for age and, therefore, ranged between passages 13 and 20. Initially, SV40-transformed normal and AT cell lines were considered for the immunoblotting experiments because of their superior doubling efficiency. However, due to an unexpected reversal of free UCRP levels in the transformed cell lines as compared with the non-transformed cell lines, it was decided to revert to working

with the non-transformed cell lines for these particular experiments.

Immunohistochemistry - The procedure was adapted for peroxidase staining of ubiquitin and UCRP (53) and provided qualitative information regarding differences in ubiquitin and/or UCRP levels between normal and AT cells. This technique provided a useful tool for detecting the striking difference in UCRP levels between normal and AT cells in stationary phase; however, it did not detect any differences in UCRP levels between normal and AT cells in log phase. Cells were always seeded at the same density ($5.5 \times 10^4/10^5$ cells) in 8-cm^2 dishes and grown for the same period of time (48 hours/5 days) to obtain log phase and stationary phase cultures, respectively. All experiments were repeated at least 3 times and the different cell lines were matched in passage number as closely as possible. Trials with normal and AT cells of different passage numbers showed the same response with respect to UCRP levels. Controls included normal and AT cells grown to log phase or confluency on coverslips and these were subjected to the immunohistochemical procedure without primary antibody. As expected, no peroxidase reaction was observed in the controls.

Flow Cytometry - To determine whether cell cycle differences in ubiquitin and UCRP distribution existed between normal and AT cells, cell cycle synchronization was carried out using the cell cycle inhibitor, aphidicolin, in normal and AT fibroblasts prior to cell sorting. Flow cytometry was carried out with Dr. P. Olive at the British Columbia Cancer Research Centre. However, the AT cells appeared to be highly sensitive to aphidicolin resulting in a high percentage of cell death. Other inhibitors were also tried including quercetin and dimethylsulfoxide, but these were equally toxic.

Immunofluorescence - Therefore, as an alternative technique for studying differences in ubiquitin conjugates and UCRP localization between normal and AT cells in different growth phases (38,53), immunofluorescence studies were undertaken. Although this technique proved to be more sensitive than

immunohistochemistry for studying differences in levels of UCRP between normal and AT cells in log phase, there was some variation between experiments. Changes in cell growth rate between experiments due to ageing, for example, may have affected the results. Cells were always seeded at the same density ($9 \times 10^4/1.25 \times 10^5$ cells) in 8-cm^2 dishes and grown for the same period of time (48 hours/5 days) to obtain log phase and stationary phase cultures, respectively. Each experiment included one normal and one AT culture and was repeated 2-3 times. Controls included the same normal and AT cultures grown to log phase or confluency on coverslips and these were subjected to the immunofluorescence procedure without primary antibody. Only background fluorescence was observed in the controls, which were given identical exposure times when photographed to the test slides. Alternatively, using pre-immune serum instead of primary antibody would constitute another, perhaps preferable, type of control.

Immunoblotting - To detect differences between the levels of conjugated and unconjugated UCRP pools in normal and AT cells, proteins were separated electrophoretically and probed using polyclonal antibodies. It was also a more quantitative assay to determine the efficacy of treating the AT cells with different concentrations of neutralizing antibodies against interferon ß and to determine the response of cells to different concentrations of interferon ß. In order to enhance the resolution of low molecular proteins, such as UCRP and LMP2, a slight modification in the composition of the running gel was introduced. All the protein samples collected in this study were electrophoresed on 15% running gels instead of on 12% running gels. Cells were always seeded at the same density ($6 \times 10^5/10^6$ cells) in 55-cm^2 dishes and grown for the same period of time (48 hours/5 days) to obtain log phase and stationary phase cultures, respectively. All experiments in which protein levels were dramatically different between normal and AT cells were performed 3 or more times to ensure reproducibility. All experiments in which protein levels were equivalent between normal and AT cells were performed 2 or more times; triplicates and doubling dilution experiments were used to demonstrate equal ratios. Control

experiments included subjecting blotted protein samples to the ECL detection procedure without incubating the blots with primary antibody. No protein bands were detected in the controls. In the case of treatment with antibodies or interferon ß, controls included untreated normal and AT cells.

ELEVATION OF INTERFERON β-INDUCIBLE PROTEINS IN ATAXIA-TELANGIECTASIA CELLS[1]

[1] A significant portion of this section has appeared in *Cancer Research*, 56: 443-447, 1996, with Arthur L. Haas and Miriam P. Rosin as co-authors.

ABSTRACT

The recently cloned ATM gene has been shown to bear considerable homology to phosphatidylinositol 3-kinases (PI3Ks) and, therefore, its product may function in signal transduction. In this study, we report constitutively elevated levels of two interferon ß-inducible proteins, ubiquitin cross-reactive protein (UCRP) and low M_r protein, LMP2, in human fibroblasts with the inherited disease ataxia-telangiectasia (AT). Using immunoblotting, it was found that a 15 kDa band representing free UCRP was hardly detectible in normal cells, while it was the predominant band in AT cells. Similarly, the expression of a 23 kDa protein, LMP2, was found to be higher in AT cells than in normal cells. Culturing three successive passages of the AT cell line in the presence of different concentrations of neutralizing antibodies against interferon ß caused partial and complete reduction, respectively, of the free UCRP and LMP2 signals to normal levels. These results indicate that UCRP and LMP2 pools may be basally elevated in AT cells due to constitutive activation of the interferon ß induction pathway and are in keeping with the recently reported constitutive activation of the NF-κB transcriptional activator in AT cells.

INTRODUCTION

Ataxia-telangiectasia (AT) is a multi-faceted autosomal recessive genetic disorder. Clinically, AT is characterized by loss of coordination and telangiectases, hypersensitivity to ionizing radiation, progressive neuronal degeneration, immunodeficiency and cancer proneness (1). Recent identification of the AT gene defect suggests that the symptoms of ataxia-telangiectasia are caused by mutation of a single gene called ATM (2). The ATM gene has been found to bear homology to several different Saccharomyces cerevisiae yeast genes including TEL1, MEC1, Tor1p and Tor2p and to the catalytic subunit of the human DNA-dependent protein kinase gene (3). The one feature common to the protein products of these genes is that they all have motifs found in phosphatidylinositol 3-kinases (PI3Ks) at their COOH-termini, as does the ATM protein. Mammalian PI3Ks are protein kinases that have been implicated as mediators of signal transduction (4). Thus, it is possible that the ATM protein also plays a role in signal transduction.

Recently, it has been reported that the NF-κB transcription factor is constitutively activated in AT cells (5). NF-κB is a member of the Rel family of transcriptional activator proteins. Stimulation of one or more signal transduction pathways involving protein kinases by certain DNA damaging agents, bacterial pathogens, viruses, and inflammatory cytokines, causes NF-κB activation and induces the expression of many genes, including interferon ß (Figure 1) (6).

In this study, we report that levels of two interferon ß-inducible proteins, ubiquitin cross-reactive protein (UCRP) and LMP2, are constitutively elevated in human fibroblasts derived from AT patients when compared to normal cells (7,8). Culturing three successive passages of an AT cell line in the presence of different concentrations of neutralizing antibody against interferon ß caused partial and

complete reduction, respectively, of the free UCRP and LMP2 immunospecific signals to normal levels. This result indicates that UCRP and LMP2 protein levels are elevated in AT cells due to abnormal interferon ß induction (Figure 1), consistent with the constitutive activation of NF-κB in AT cells, measured as the binding of NF-κB to its κB recognition site (5). However, we observed no differences in expression of the p65, p50, and IκB-α components of the NF-κB activation pathway between AT and normal cells suggesting that some other element of this pathway may be dysfunctional. Thus, there appears to be constitutive activation of the interferon ß gene in AT cells as a result of a defect in some aspect of the NF-κB activation pathway.

MATERIALS AND METHODS

Chemicals. Sodium azide, bovine serum albumin, sodium dodecyl sulphate (SDS), Ponceau S solution, and molecular weight standard (14 kDa) were purchased from Sigma. Tween-20, Tris, Temed, ammonium persulphate, bromophenol blue, ß-mercaptoethanol, acrylamide, bisacrylamide, broad range molecular weight standards, and Coomassie Blue R250 were from Bio-Rad. Glycerol was from BDH. The ECL detection reagent kit and hyperfilm for ECL visualization was obtained from Amersham. Human recombinant interferon ß-1b was generously provided by Berlex Laboratories for these experiments.

Antibodies. As previously described, rabbit anti-ubiquitin and anti-UCRP polyclonal antibodies were generated against SDS-denatured ubiquitin and recombinant mature human UCRP, respectively, and affinity purified (9,10). The LMP2 polyclonal antibody was very kindly provided by Dr. Keiji Tanaka (Institute

for Enzyme Research, Tokushima, Japan). Antibodies to p65 and p50 were obtained from Upstate Biotechnology Incorporated (Lake Placid, NY) and the antibody to IκB-α was purchased from Santa Cruz Biotechnology (Santa Cruz, CA). Rabbit anti-human interferon ß neutralizing antibody was purchased from Lee Biomolecular (San Diego, CA).

Cell Lines and Culture. The primary cell cultures of normal (5757) and AT (1588) non-transformed human fibroblasts were obtained from the Coriell Cell Repositories (Camden, NJ). Fibroblast cultures were grown in Dulbecco's modified Eagle media (D-MEM, Flow, McLean, VA) supplemented with 15% heat-inactivated fetal calf serum (FCS, Gibco, Grand Island, NY), penicillin (100 units/ml) and streptomycin (100 μg/ml). All stock cultures were maintained in 75-cm^2 culture flasks at 37°C in incubators with a 5% CO_2/95% air atmosphere. In all experiments, the indicated concentration of anti-interferon ß was added directly to the culture media during passaging or media change.

Western blotting. Log and stationary cultures of 5757 and 1588 primary fibroblasts were rinsed with PBS, followed by lysis in Laemmli buffer [119 mM Tris, pH 6.8, 20% glycerol, 4% SDS, 5% vol/vol ß-mercaptoethanol] (11). The samples were sonicated for 20 seconds and boiled for 4 minutes. The protein content of each sample was determined in duplicate using a standard Coomassie dye binding assay according to Bradford (12). SDS-PAGE was performed on 15% acrylamide slab gels (0.1% bisacrylamide, 11 cm height). Equal amounts of protein (200 μg) were loaded in each lane. For immunodetection, the samples were electrophoretically transferred to a polyvinylidene difluoride (PVDF) membrane (Bio-Rad) using a Tris-glycine buffer (25 mM Tris, pH 8.3, 192 mM glycine). The transfer was carried out at a constant current of 350 mA for 2 hours at 4°C. Proteins bands were visualized on the blot with Ponceau red [0.1% Ponceau S (w/v) in 5% acetic acid (v/v)].

Nonspecific binding was blocked by incubating the blots with 5% non-fat dried milk in Tris-buffered saline with Tween-20 [TTBS; 50 mM Tris, pH 7.4, 155 mM NaCl, 0.5% (vol/vol) Tween-20] for 60 minutes. The blots were rinsed with TTBS and then incubated with the primary antibody in 1% bovine serum albumin in TTBS (0.5% sodium azide). After 3 washes lasting 10 minutes each in TTBS, the blots were incubated with protein A-peroxidase (1:5000) in 1% bovine serum albumin in TTBS for 90 minutes. The peroxidase activity was visualized using luminol (ECL, Amersham). The exposure time was 30 seconds to 1 minute. All steps of the immunodetection procedure were carried out at room temperature with gentle shaking, except for the incubation with the primary antibody which was performed overnight at 4°C. The ubiquitin and UCRP antiserum (9,10) was used at a dilution of 1 μg/ml. The LMP2 antiserum was used at a 1/500 dilution. The p65, p50, and IκB-α antisera were all used at a dilution of 1 μg/ml.

RESULTS

Elevation of UCRP in AT Cells. Like AT cells, certain yeast cell cycle mutants, such as the S. cerevisiae RAD6 mutant, are deficient in DNA repair following X-irradiation. The RAD6 gene encodes a ubiquitin-conjugating E2 enzyme (13). Therefore, initially, Western blot analysis was used to test for any differences in ubiquitin levels that might arise between normal and AT cells due to a defect in ubiquitin conjugation (Fig.2a.) No difference in ubiquitin levels was observed. However, the affinity purified anti-ubiquitin probe used in these studies bound to a 15 kDa band in the AT cells (Fig.2a, lanes 2,4), but not in the normal cells (Fig.2a, lanes 1,3), which most likely represented unconjugated UCRP (9). This was

followed by experiments in which normal and AT protein samples were probed with an affinity purified anti-UCRP antibody. The results obtained confirmed that a 15 kDa band representing UCRP was abundant in the AT cells while it was barely detectible in the normal cells (Fig.3a).

SDS-PAGE was performed on total proteins obtained from normal and AT fibroblast cell lines, in both log and stationary phases, and the Western blots were probed with an affinity purified polyclonal antibody directed against UCRP as specified in Materials and Methods.

In normal log phase cells, the UCRP antibody recognized one major band of 100 kDa (Fig.3a, lane 1). In normal stationary phase cells (Fig.3a, lane 3), the UCRP antibody also recognized a protein species of 55 kDa in addition to the 100 kDa protein band. In contrast, in AT log and stationary phase cells (Fig.3a, lane 2), three major protein species of an apparent molecular weight of 100, 55, and 15 kDa were recognized by the UCRP antibody. The 15 kDa protein band corresponded to free UCRP. The UCRP antibody also recognized less abundant protein bands of high molecular weight in the stationary cells.

Although, the free UCRP protein band of 15 kDa was present in different amounts in normal cell cultures (see Fig.3a, lanes 1,3 and Figs.4a & 5a, lane 1), free UCRP was always more abundant in AT cells than in normal cells, especially in stationary phase cultures.

Elevation of LMP2 in AT Cells. As UCRP is inducible by interferon ß treatment, it was of interest to find out whether other interferon ß-inducible proteins were also elevated in AT cells as compared with normal cells. SDS-PAGE was performed on total proteins obtained from normal and AT fibroblast cell lines, in both log and stationary phases, and the Western blots were probed with a polyclonal antibody directed against LMP2 as specified in Materials and Methods.

The LMP2 antibody recognized one major band at approximately 23 kDa in normal log and stationary cells (Fig.3b, lanes 1,3). One major protein species of approximately 23 kDa was also recognized by the LMP2 antibody in both AT log and stationary cells (Fig.3b, lanes 2,4).

The LMP2 protein was recognized to different extents in normal cultures (see Fig.3b, lanes 1,3 and Figs.4b,5c & 5d, lane 1) but, as with UCRP, the LMP2 appeared to be more abundant in AT than in normal cells. This contrast was more pronounced between log than stationary phase cultures.

Interferon ß Neutralization Blocks UCRP and LMP2 in AT cells. To determine whether the elevation of interferon ß-inducible proteins in AT cells resulted from constitutive interferon ß production, UCRP and LMP2 levels were measured following anti-interferon ß treatment. Normal and AT cells in stationary phases were treated with anti-interferon ß over a period of three generations as specified in Materials and Methods to neutralize any interferon ß generated by the cells.

In the first experiment (Fig.4), the anti-interferon ß was used at a concentration of 10 neutralizing units per ml. After treatment with anti-interferon ß, the 15 kDa band representing the free UCRP pool was slightly reduced in the normal cells as compared to the control (Fig.4a, lanes 3 and 1, respectively), while it was significantly reduced in the AT cells as compared to the control (Fig.4a, lanes 4 and 2, respectively). After treatment with anti-interferon ß, there was no decrease in the 23 kDa band representing LMP2 in the normal cells as compared to the control (Fig.4b, lanes 3 and 1, respectively), while there was a decrease in the LMP2 level in the AT cells as compared to the control (Fig.4b, lanes 4 and 2, respectively).

In the second experiment (Fig.5a & 5b), the anti-interferon ß was used at a concentration of 100 neutralizing units per ml. As before, following the anti-

interferon ß treatment, the free UCRP pool was unchanged in the normal cells (Fig.5a, lane 3), but was greatly reduced in the AT cells (Fig.5a, lane 4). Similarly, the LMP2 pool remained unchanged in the normal cells (Fig.5b, lane 3), but was significantly reduced in the AT cells (Fig.5b, lane 4).

Interferon ß Induction of UCRP and LMP2 is Normal in AT Cells. In order to test whether AT cells are responsive to interferon ß and whether inhibition by the anti-interferon ß antibody can be overcome by high levels of interferon, the cells were exposed to various concentrations of interferon ß. Previous studies have shown that interferon ß treatment induces UCRP and its conjugates in cultured human cells (9). As expected, in normal and AT stationary cells treated with interferon ß at concentrations of 10 IU/ml (Fig.5c, lanes 1 and 2, respectively), 100 IU/ml (Fig.5c, lanes 5 and 6, respectively), and 1000 IU/ml (Fig.5c, lanes 9 and 10, respectively) for 24 hours, UCRP and its conjugates were induced as compared to the untreated cells (Fig.5a, lanes 1 and 2, respectively). In normal and AT stationary cells pre-treated with anti-interferon ß (100 neutralizing units/ml) for 3 generations, treatment with interferon ß at a dose of 10 IU/ml (Fig.5c, lanes 3 and 4, respectively) and 100 IU/ml (Fig.5c, lanes 7 and 8, respectively) did not cause any visible UCRP induction demonstrating neutralization by the antibody. However, treatment with interferon ß at a dose of 1000 IU/ml of normal and AT stationary cells pre-treated with anti-interferon ß (100 neutralizing units/ml) for 3 generations caused induction of UCRP and its conjugates (Fig.5c, lanes 11 and 12, respectively) as compared to the untreated cells (Fig.5a, lanes 1 and 2, respectively) demonstrating inability of the antibody to neutralize higher concentrations of interferon ß.

In normal and AT stationary cells treated with interferon ß at concentrations of 10 IU/ml (Fig.5d, lanes 3 and 4, respectively), 100 IU/ml (Fig.5d, lanes 5 and 6,

respectively), and 1000 IU/ml (Fig.5d, lanes 7 and 8, respectively) for 24 hours, LMP2 was induced as compared to the controls (Fig.5d, lanes 1 and 2, respectively) demonstrating that it is an interferon ß responsive protein in AT cells.

p65, p50, and IκB-α Levels are Normal in AT Cells. In order to test whether the apparent increase in expression of the interferon ß gene in AT cells is caused by changes in the expression of components of the NF-κB activation pathway, the levels of p65, p50, and IκB-α were compared in normal and AT cells. SDS-PAGE was performed on total proteins obtained from normal and AT fibroblast cell lines in stationary phase and the Western-blots were probed with a polyclonal antibody directed against p65, p50, or IκB-α as specified in Materials and Methods.

In normal and AT stationary phase cells, the p65 antibody recognized an equivalent band of 65 kDa (Fig.6a, lanes 1 and 2, respectively), the p50 antibody recognized an equivalent band of 50 kDa (Fig.6b, lanes 1 and 2, respectively), and the IκB-α antibody recognized an equivalent band of 42 kDa (Fig.6c, lanes 1 and 2, respectively). No differences in expression of these proteins in AT compared to normal cells were evident.

DISCUSSION

The results obtained show that free UCRP levels are constitutively elevated in AT cells. Two significant 100 kDa and 55 kDa adducts that are present in normal cells are also present in the AT cells but are less abundant than the 15 kDa free UCRP species. Moreover, variations in the UCRP pools appear to be growth phase dependent since free UCRP is found to be more abundant in stationary than in log AT cells. In contrast, most of the UCRP in both log and stationary normal cells

appears to exist as either the 100 kDa or 55 kDa adduct while free UCRP is barely detectible. This suggests a difference in the dynamics of UCRP pools between AT and normal cells. However, cell synchronization studies would be required to identify the precise nature of these variations according to each stage of the cell cycle. LMP2 levels are also constitutively elevated in AT cells. This contrast is more pronounced between log phase than stationary phase AT and normal cells, as LMP2 levels are less abundant in log phase than in stationary normal cells while there does not appear to be much change in the LMP2 levels of log and stationary AT cells. Once again, this indicates the possibility that variations in LMP2 pools may be growth phase dependent and that there is a difference in the dynamics of LMP2 pools between AT and normal cells.

The induction of UCRP, UCRP conjugates and LMP2 following 24 hours of interferon ß treatment at doses of 10 IU/ml, 100 IU/ml, and 1000 IU/ml appears to be normal in AT cells. Furthermore, culturing in the presence of anti-interferon ß for 3 generations at concentrations of 10 neutralizing units/ml and 100 neutralizing units/ml caused partial and complete reduction, respectively, of the elevated free UCRP and LMP2 in AT cells to normal levels. Taken together, these results suggest that interferon ß-inducible proteins are elevated in AT cells due to interferon autoinduction, indicating that AT but not normal cells are producing interferon ß.

The results presented above indicate that AT cells exhibit constitutive activation of interferon ß gene regulation resulting in basally elevated levels of the interferon-inducible proteins, UCRP and LMP2. The transcription factor, NF-κB, is required for the transcriptional activation of the interferon ß gene since interferon ß gene induction can be blocked by NF-κB antisense RNA (14,15). Therefore, the elevation of UCRP observed in AT cells is consistent with constitutive NF-κB activation resulting in continuous induction of the interferon ß gene.

However, it appears that the abnormal induction of the interferon ß gene is not caused merely by changes in the expression of the p65 or p50 NF-κB subunits or in the IκB-α inhibitory protein in AT cells.

The interferons are a family of molecules (α,ß, and γ) which induce a wide range of biological functions in cells including antiviral, antigrowth and immunomodulatory activities. A variety of proteins or mRNAs are known to be induced by interferon ß treatment including UCRP and LMP2, while others are downregulated. Interferon treatment inhibits the expression of certain growth competence-related genes or oncogenes, such as c-myc and ras (16,17,18). Moreover, interferon ß has been reported to decrease the mRNA expression of several genes that control entry into S phase, including cyclin A and cyclins D1 and D2 (19). It has also been shown that p53 and interferon ß can work in concert to produce a G0/G1 type of arrest in M1 cells (19). The role of p53 in arresting cycling cells at the G1-S boundary in response to DNA damage following X-ray exposure has been well documented (20) and this complementation between p53 and interferon ß may represent another step in the pathway. The fact that the interferons retard the growth and proliferation of tumour cells as well as normal cells by prolonging the cell cycle has been successfully exploited to various degrees in providing the first effective cancer therapy (21,22,23,24). However, interferon expression has also been linked to certain growth stimulating processes. For instance, interferon γ has been found to induce the expression of certain proteasomal subunits including LMP2 (8,25,26). Proteasomes are ubiquitous, multifunctional enzymes involved in the ATP-dependent degradation of proteins conjugated with ubiquitin (27,28). The unusually high expression of proteasomes has been implicated in development, cell growth and proliferation, viral transformation, and cancer (29,30,31,32). Recently, UCRP has been shown to act extracellularly as a cytokine in the subsequent induction of

interferon γ and thus to indirectly modulate the immune response in humans (33). Thus, one possibility is that the constitutive elevation of free UCRP and LMP2 together could result in an increase of proteasome activity in AT cells which could be linked, in part, to the induction of cancer in this disease.

In conclusion, it is important to note the possible clinical application of this research. If the ATM gene causes activation of a pathway leading to constitutive interferon ß gene induction, then treatment with anti-interferon ß could help to suppress the possibly damaging effects of this continuous interferon induction by reducing cellular interferon levels to a minimum. However, at present there is no evidence to suggest that the elevation of UCRP and LMP2 observed in AT cells is connected to the etiology of cancer proneness associated with this disease.

ACKNOWLEDGEMENTS

We would like to thank Dr. Silia Chadan for her valuable suggestions on the immunoblotting technique and helpful criticism of the manuscript. We would also like to thank Dr. Keiji Tanaka for generously providing the LMP2 antibody used in this study.

REFERENCES

1. McKinnon, P.J. Ataxia-telangiectasia: an inherited disorder of ionizing-radiation sensitivity in man. Hum. Genet., 75: 197-208, 1987.

2. Savitsky, K., Bar-Shira, A., Shlomit, G., Rotman, G., Ziv, Y., Vanagaite, L., Tagle, D.A., Smith, S., Uziel, T., Sfez, S., Askenazi, M., Pecker, I., Frydman, M., Harnik, R., Patanjali, S.R., Simmons, A., Clines, G.A., Sartiel, A., Gatti, R.A., Chessa, L., Sanal, O., Lavin, M.F., Jaspers, N.G.J., Taylor, M.R., Arlett, C.F., Miki, T., Weissman, S.W Lovett, M., Collins, F.S. and Shiloh, Y. A single ataxia telangiectasia gene with a product similar to PI-3 kinase. Science, 268: 1749-1753, 1995.

3. Zakian, V.A. ATM-related genes: what do they tell us about functions of the human gene? Cell, 82: 685-687, 1995.

4. Hiles, I.D., Otsu, M., Volinia, S., Fry, M.J., Gout, I., Dhand, R., Panayotou, G., Ruiz- Larrea, F., Thompson, A., Totty, N.F., Hsuan, J.J., Courtneidge, S.A., Parker,P.J., and Waterfield, M.D. Phosphatidylinositol 3-Kinase: Structure and Expression of the 110 kd Catalytic Subunit. Cell 70: 419-429, 1992.

5. Jung, M., Zhang, Y., Lee, S. and Dritschilo, A. Correction of radiation sensitivity in ataxia-telangiectasia cells by a truncated IκB-α. Science, 268: 1619-1621, 1995.

6. Thanos, D. and Maniatis, T. NF-κB: A lesson in family values. Cell, 80: 529-532, 1995.

7. Haas, A.L., Ahrens, P., Bright, P.M., and Ankel, H. Interferon induces a 15-kilodalton protein exhibiting marked homology to ubiquitin. J. Biol. Chem., 262 (23): 11315-11323, 1987.

8. Aki, M., Shimbara, N., Takashina, M., Akiyama, K., Kagawa, S., Tamura, T., Tanahashi, N., Yoshimura, T., Tanaka, K. and Ichihara, A. Interferon γ induces different subunit organizations and functional diversity of proteasomes. J. Biochem., 115: 257-269, 1994.

9. Loeb, K.R. and Haas, A.L. The interferon-inducible 15-kDa ubiquitin homolog conjugates to intracellular proteins. J. Biol. Chem., 267(11): 7806-7813, 1992.

10. Haas, A.L. and Bright, P.M. The immunochemical detection and quantitation of intracellular ubiquitin-protein conjugates. J. Biol. Chem., 260(23): 12464-12473, 1985.

11. Laemmli, U.K. Cleavage of structural proteins during the assembly of the head of bacteriophage T4. Nature, 227: 680-685, 1970.

12. Bradford, M. A rapid and sensitive method for the quantitation of microgram quantities of protein by an improved protein-dye binding assay. Anal. Biochem., 72: 248-254, 1976.

13. Jentsch, S., McGrath, J.P., and Varshavsky, A. The yeast DNA repair gene RAD6 encodes a ubiquitin-conjugating enzyme. Nature, 329: 131-134, 1987.

14. Thanos, D. and Maniatis, T. Identification of the rel family members required for virus induction of the human beta interferon gene. Mol. & Cell. Biol., 15(1); 152-164, 1995.

15. Thanos, D. and Maniatis, T. The high mobility group protein HMG I(Y) is required for NF-κB-dependent virus induction of the human IFN-ß gene. Cell, 71:777-789, 1992.

16. Borden, E.C. Interferons: pleiotropic cellular modulators. Clin. Immunol. & Immunopathol., 62(1): S18-S24, 1992.

17. Sen, G.C. and Lengyel,P. The interferon system. J. Biol. Chem., 267(8):5017-5020, 1992.

18. Kerr,I.M. and Stark,G.R. The control of interferon-inducible gene expression. Febs Letts., 285(2): 194-198, 1991.

19. Levy, N., Yonish-Rouach, E., Oren, M. and Kimchi, A. Complementation by wild-type p53 of interleukin-6 effects on M1 cells: induction of cell cycle exit and cooperativity with c-myc suppression. Mol. & Cell. Biol., 13(12): 7942-7952, 1993.

20. Zhan, Q., Bae, I., Kastan, M.B. and Fornace, A. J. The p53-dependent γ-ray response of GADD45. Cancer Res., 54: 2755-2760, 1994.

21. Schiller, J.H., Storer, B., Paulnock, D.M., Brown, R.R., Datta, S.P., Witt, P.L. and Borden, E.C. A direct comparison of biological response modulation and clinical side effects by interferon-beta, interferon-gamma, or the combination of interferons beta and gamma in humans. J. Clin. Invest., 86: 1211-1221, 1990.

22. Itri,L.M. The interferons. Cancer Suppl., 70(4): 940-944, 1992.

23. Borden, E.C. Interferons - expanding therapeutic roles. New Engl. J. Med., 326(22): 1491-1493, 1992.

24. Talpaz, M., Kantarjian, H., Kurzrock, R., Trujillo, J.M., and Gutterman, J.U. Interferon-alpha produces sustained cytogenetic responses in chronic myelogenous leukemia. Annals Int. Med., 114: 532-538, 1991.

25. Ortiz-Navarrete, V., Seelig, A., Gernold, M., Frentzel, S., Kloetzel, P.M. and Hammerling, G.J. Subunit of the '20S' proteasome (multicatalytic proteinase) encoded by the major histocompatibility complex. Nature, 353: 662-664, 1991.

26. Kelly, A., Powis, S.H., Glynne, R., Radley, E., Beck, S. and Trowsdale, J. Second proteasome-related gene in the human MHC class II region. Nature, 353: 667-668, 1991.

27. Goldberg, A.L. and Rock, K.L. Proteolysis, proteasomes and antigen presentation. Nature, 357: 375-379, 1992.

28. Tanaka, K., Tamura, T., Yoshimura, T. and Ichihara, A. Proteasomes: protein and gene structures. New Biol., 4(3): 173-187, 1992.

29. Ichihara, A., Tanaka, K., Andoh,T. and Shimbara,N. Regulation of proteasome expression in developing and transformed cells. Advan. Enzyme Regul., 33: 173-180, 1993.

30. Shimbara, N., Orino, E., Sone, S., Ogura,T., Takashina, M., Shono, M., Tamura, T., Yasuda,H., Tanaka,K. and Ichihara,A. Regulation of gene expression of proteasomes (multi-protease complexes) during growth and differentiation of human hematopoietic cells. J. Biol. Chem., 267(25): 18100-18109, 1992.

31. Kumatori, A.,T anaka, K., Inamura, N., Sone, S., Ogura, T., Matsumoto, T., Tachikawa, T., Shin, S. and Ichihara, A. Abnormally high expression of proteasomes in human leukemic cells. Proc. Natl. Acad. Sci. USA, 87: 7071-7075, 1990.

32. Kanayama, H., Tanaka, K., Aki, M., Kagawa, S., Miyaji, H., Satoh, M., Okada,F., Sato, S., Shimbara, N. and Ichihara, A. Changes in expressions of proteasome and ubiquitin genes in human renal cancer cells. Cancer Res., 51: 667-6685, 1991.

33. D'Cunha, J., Knight, E., Haas, A.L. Truitt, R.L. and Borden, E.C. Immunoregulatory properties of ISG15, an interferon-induced cytokine. Proc. Natl. Acad. Sci. USA, 93: 211-215, 1996.

FIGURE LEGENDS

Figure 1. Hypothetical Pathway for NF-κB Activation. This diagram represents a hypothetical pathway for NF-κB activation and its subsequent induction of the interferon ß gene in normal (N) and AT cells [adapted from (6)]. The question marks on the AT side of the diagram denote points in the pathway that may be affected by the ATM gene resulting in the constitutive activation of NF-κB.

Figure 2a & b. Immunoblot Analysis of Ubiquitin in Log and Stationary Normal and AT Fibroblasts. Normal (5757) and AT (1588) fibroblast cultures were grown to log or stationary phase, rinsed twice with PBS, and solubilized into SDS sample buffer. Parallel samples of AT and normal fibroblast extracts were resolved by SDS-PAGE and either stained with Coomassie blue dye (panel b), or transferred to a PVDF membrane, and probed with ubiquitin antiserum (panel a). The arrow to the right of panel a denotes the position of free UCRP. **Lane 1.** untreated normal fibroblasts in log phase; **Lane 2.** untreated AT fibroblasts in log phase; **Lane 3.** untreated normal fibroblasts in stationary phase **Lane 4.** untreated AT fibroblasts in stationary phase.

Figure 3a. Immunoblot Analysis of UCRP in Log and Stationary Normal and AT Fibroblasts. Normal (5757) and AT (1588) fibroblast cultures were grown to log or stationary phase, rinsed twice with PBS, and solubilized into SDS sample buffer. Parallel samples of AT and normal fibroblast extracts were resolved by SDS-PAGE, transferred to a PVDF membrane, and probed with UCRP antiserum. The arrow to the right of panel a denotes the position of free UCRP. **Lane 1.** untreated normal fibroblasts in log phase; **Lane 2.** untreated AT fibroblasts in log phase; **Lane 3.** untreated normal fibroblasts in stationary phase **Lane 4.** untreated AT fibroblasts in stationary phase.

Figure 3b. Immunoblot Analysis of LMP2 in Log and Stationary Normal and AT Fibroblasts. Normal (5757) and AT (1588) fibroblast cultures were grown to log or stationary phase, treated exactly as described in Figure 1b and were then probed with LMP2 antiserum. The arrow to the left of panel b denotes the position of LMP2. **Lane 1.** untreated normal fibroblasts in log phase; **Lane 2.** untreated AT fibroblasts in log phase; **Lane 3.** untreated normal fibroblasts in stationary phase; **Lane 4.** untreated AT fibroblasts in stationary phase.

Figure 4a. Immunoblot Analysis of UCRP in Normal and AT Fibroblasts Following Anti-interferon ß Treatment (10 neutralizing units/ml). Normal (5757) and AT (1588) cell cultures were passaged and cultured in the presence of anti-interferon ß (10 neutralizing units/ml) for 3 generations. The normal and AT fibroblasts were grown to stationary phase and treated as described in Figure 1. **Lane 1.** untreated normal fibroblasts; **Lane 2.** untreated AT fibroblasts; **Lane 3.** treated normal fibroblasts; **Lane 4.** treated AT fibroblasts.

Figure 4b. Immunoblot Analysis of LMP2 in Normal and AT Fibroblasts Following Anti-interferon ß Treatment (10 neutralizing units/ml). Normal (5757) and AT (1588) cell cultures were passaged and cultured in the presence of anti-interferon ß (10 neutralizing units/ml) for 3 generations. The normal and AT fibroblasts were grown to stationary phase and treated as described in Figure 1. **Lane 1.** untreated normal fibroblasts; **Lane 2.** untreated AT fibroblasts; **Lane 3.** treated normal fibroblasts; **Lane 4.** treated AT fibroblasts.

Figure 5a. Immunoblot Analysis of UCRP in Normal and AT fibroblasts Following Anti-interferon ß Treatment (100 neutralizing units/ml). Normal (5757) and AT (1588) cell cultures were passaged and cultured in the presence of anti-interferon ß (100 neutralizing units/ml) for 3 generations. Then, treated and untreated cells were grown to stationary phase and subjected to the same procedure as described in Figure 1. **Lane 1.** untreated normal fibroblasts; **Lane 2.** untreated AT fibroblasts; **Lane 3.** treated normal fibroblasts ; **Lane 4.** treated AT fibroblasts

Figure 5b. Immunoblot Analysis of LMP2 in Normal and AT fibroblasts Following Anti-interferon ß Treatment (100 neutralizing units/ml). Normal (5757) and AT (1588) cell cultures were passaged and cultured in the presence of anti-interferon ß (100 neutralizing units/ml) for 3 generations. Then, treated and untreated cells were grown to log phase and subjected to the same procedure as described in Figure 1. **Lane 1.** untreated normal fibroblasts; **Lane 2.** untreated AT fibroblasts; **Lane 3.** treated normal fibroblasts; **Lane 4.** treated AT fibroblasts

Figure 5c. Immunoblot Analysis of UCRP in Normal and AT fibroblasts Following Anti-interferon ß Treatment and Interferon ß Treatment. Normal (5757) and AT (1588) cell cultures were passaged and cultured in the presence of anti-interferon ß (100 neutralizing units/ml) for 3 generations. Then, treated and untreated cells were grown to stationary phase and incubated with interferon ß (10 IU/ml, 100 IU/ml, or 1000 IU/ml) for 24 hours followed by the same procedure as described in Figure 1. **Lane 1.** normal fibroblasts treated with interferon ß (10 IU/ml); **Lane 2.** AT fibroblasts treated with interferon ß (10 IU/ml);
Lane 3. normal fibroblasts cultured in anti-interferon ß (100 neutralizing units/ml) and treated with interferon ß (10 IU/ml); **Lane 4.** AT fibroblasts cultured in anti-interferon ß (100 neutralizing units/ml) and treated with interferon ß (10 IU/ml); **Lane 5.** normal fibroblasts treated with interferon ß (100 IU/ml); **Lane 6.** AT fibroblasts treated with interferon ß (100 IU/ml); **Lane 7.** normal fibroblasts cultured in anti-interferon ß (100 neutralizing units/ml) and treated with interferon ß (100 IU/ml); **Lane 8.** AT stationary fibroblasts cultured in anti-interferon ß (100 neutralizing units/ml) and treated with interferon ß (100 IU/ml); **Lane 9.** normal fibroblasts treated with interferon ß (1000 IU/ml); **Lane 10.** AT fibroblasts treated with interferon ß (1000 IU/ml); **Lane 11.** normal fibroblasts cultured in anti-interferon ß (100 neutralizing units/ml) and treated with interferon ß (1000 IU/ml);

Lane 12. AT fibroblasts cultured in anti-interferon ß (100 neutralizing units/ml) and treated with interferon ß (1000 IU/ml).

Figure 5d. Immunoblot Analysis of LMP2 in Normal and AT fibroblasts Following Interferon ß Treatment. Normal (5757) and AT (1588) cell cultures were grown to stationary phase and incubated with interferon ß (10 IU/ml, 100 IU/ml, or 1000 IU/ml) for 24 hours followed by the same procedure as described in Figure 1. **Lane 1.** normal fibroblasts; **Lane 2.** AT fibroblasts; **Lane 3.** normal fibroblasts treated with interferon ß (10 IU/ml); **Lane 4.** AT fibroblasts treated with interferon ß (10 IU/ml) **Lane 5.** normal fibroblasts treated with interferon ß (100 IU/ml); **Lane 6.** AT fibroblasts treated with interferon ß (100 IU/ml); **Lane 7.** normal fibroblasts treated with interferon ß (1000 IU/ml); **Lane 8.** AT fibroblasts treated with interferon ß (1000 IU/ml).

Figure 6a. Immunoblot Analysis of p65 in Normal and AT Fibroblasts. Normal (5757) and AT (1588) cell cultures were grown to stationary phase and subjected to the same procedure as described in Figure 1. **Lane 1.** normal fibroblasts;
Lane 2. AT fibroblasts.

Figure 6b. Immunoblot Analysis of p50 in Normal and AT Fibroblasts. Normal (5757) and AT (1588) cell cultures were grown to stationary phase and subjected to the same procedure as described in Figure 1. **Lane 1.** normal fibroblasts;
Lane 2. AT fibroblasts.

Figure 6c. Immunoblot Analysis of IκB-α in Normal and AT Fibroblasts. Normal (5757) and AT (1588) cell cultures were grown to stationary phase and subjected to the same procedure as described in Figure 1. **Lane 1.** normal fibroblasts; **Lane 2.** AT fibroblasts.

Figure 1. Hypothetical Pathway for NF-κB Activation[1]

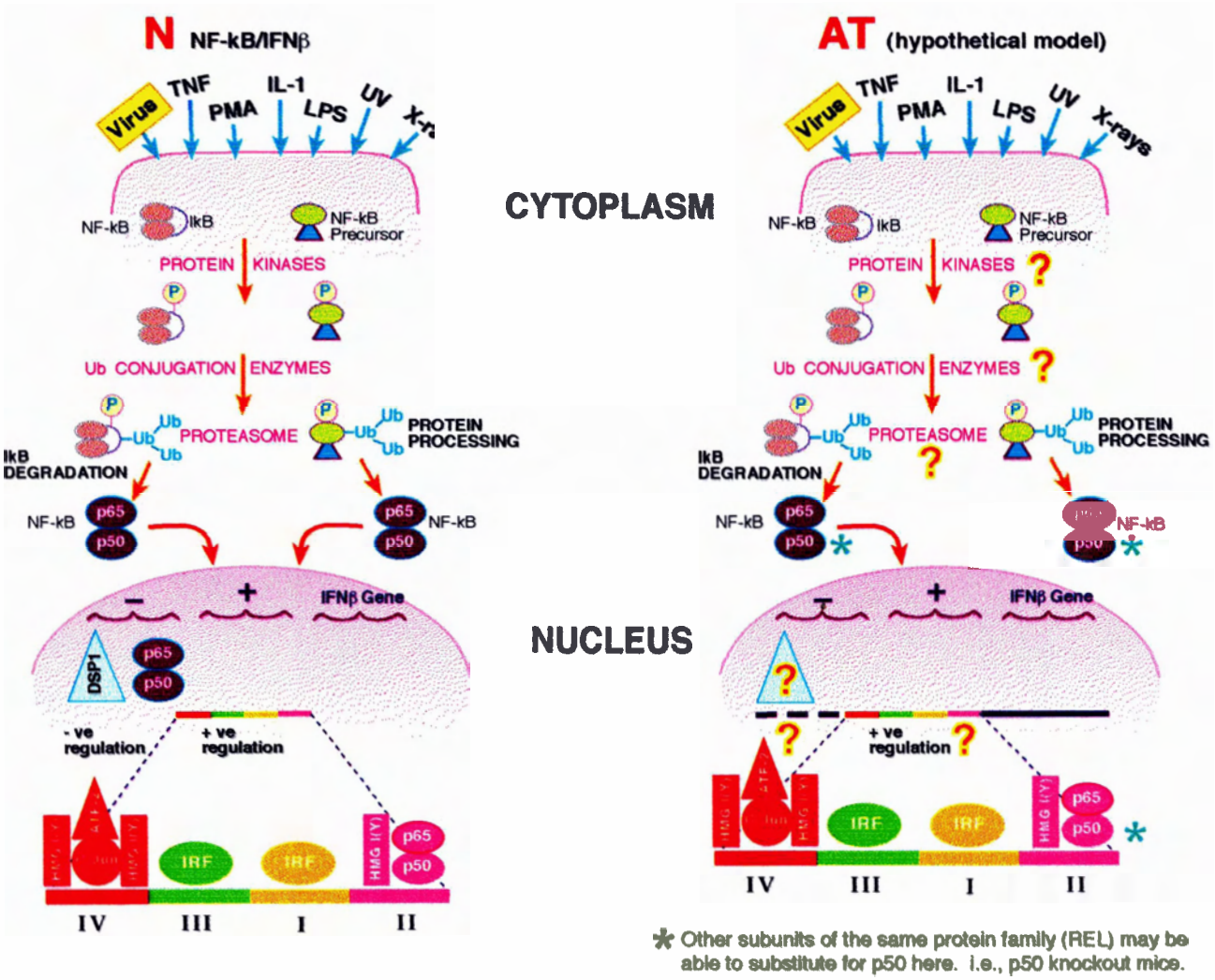

* Other subunits of the same protein family (REL) may be able to substitute for p50 here. i.e., p50 knockout mice.

[1]Adapted from reference [6]

Figure 2.

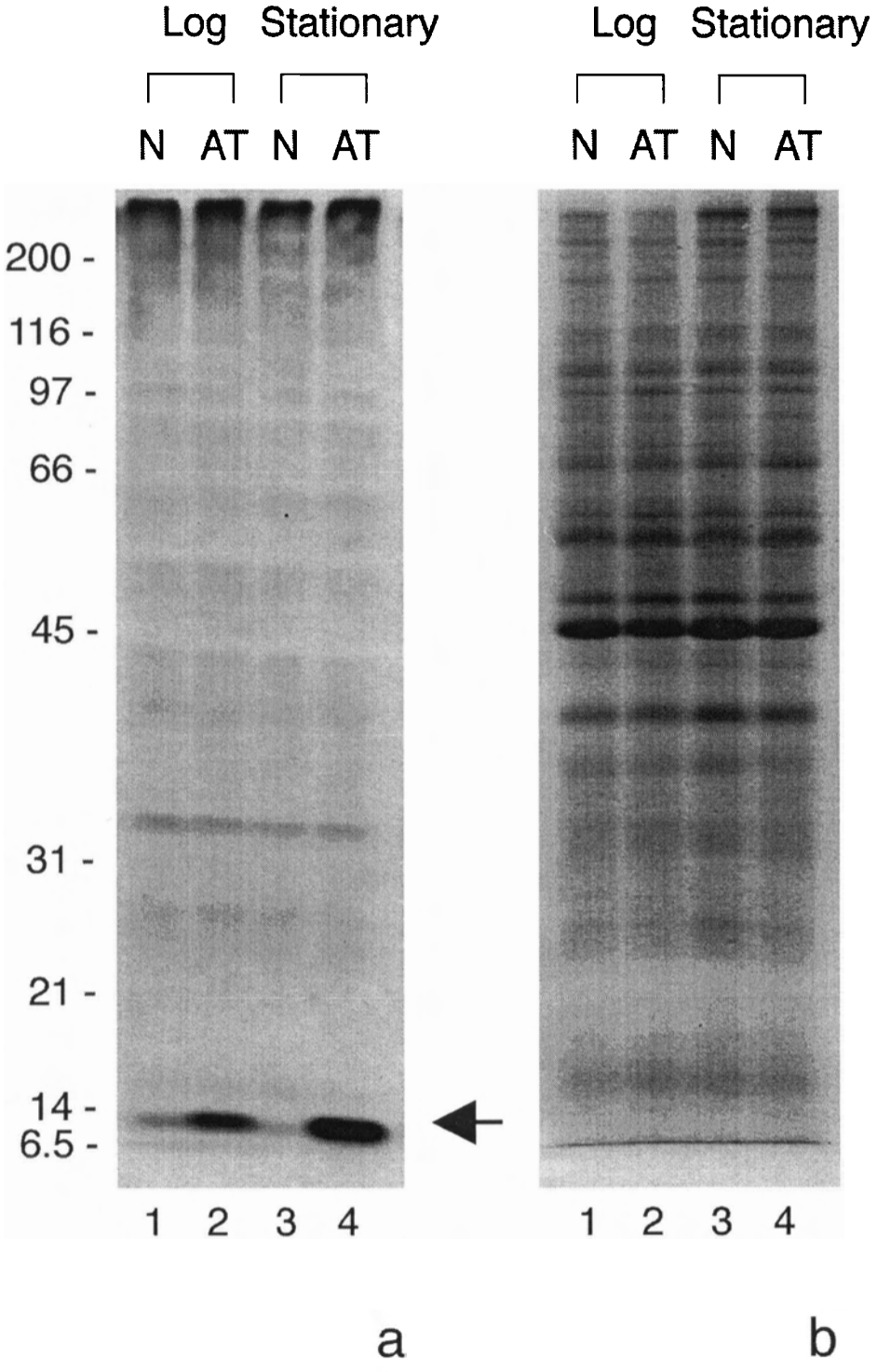
Log
Stationary
Log
Stationary
N
AT
N
AT
N
AT
N
AT
200 -
116 -
97 -
66 -
45 -
31 -
21 -
14 -
6.5 -
1
2
3
4
1
2
3
4
a
b

Figure 3.

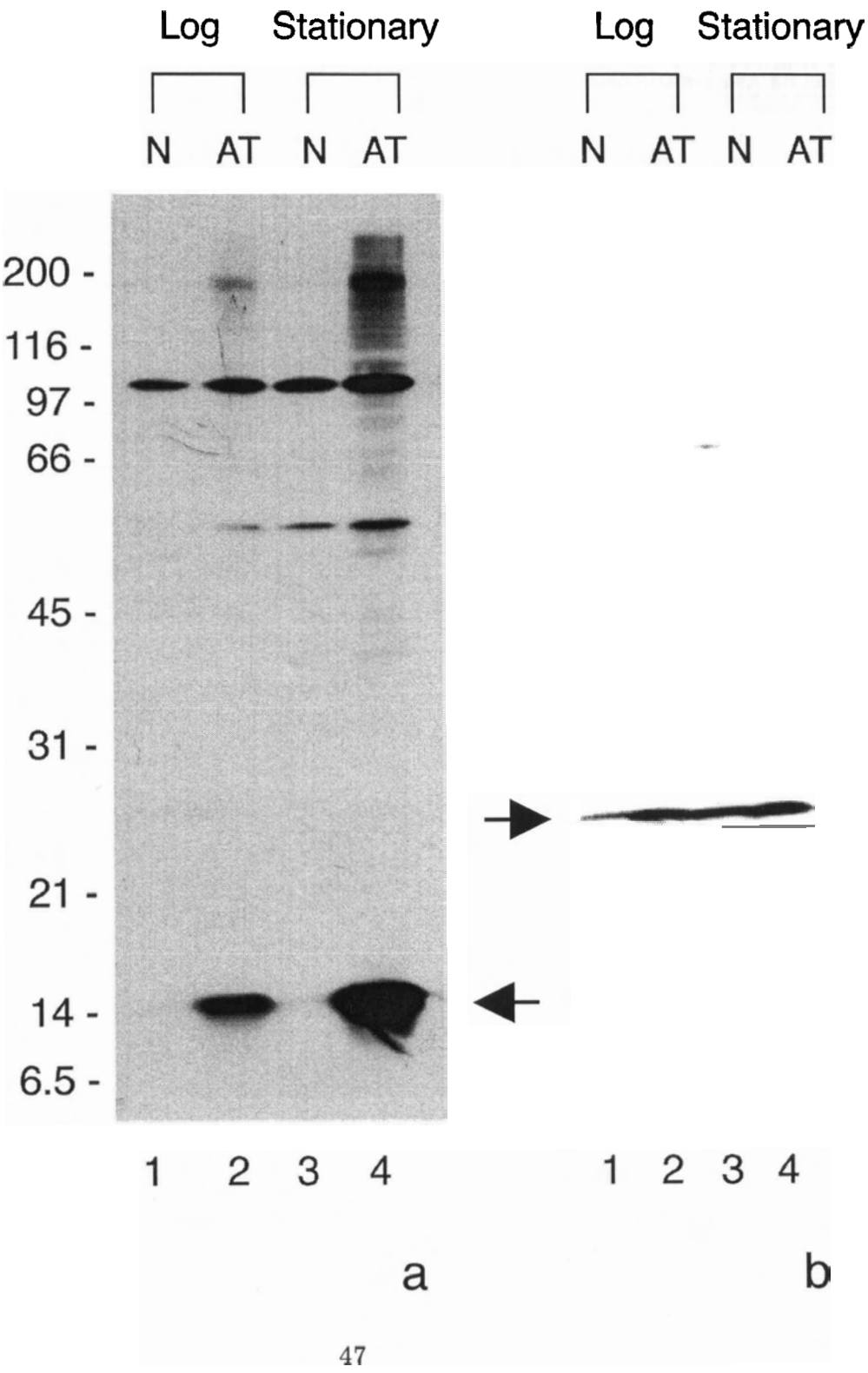
Log
Stationary
Log
Stationary
N
AT
N
AT
N
AT
N
AT
200 -
116 -
97 -
66 -
45 -
31 -
21 -
14 -
6.5 -
1
2
3
4
1
2
3
4
a
b

Figure 4.

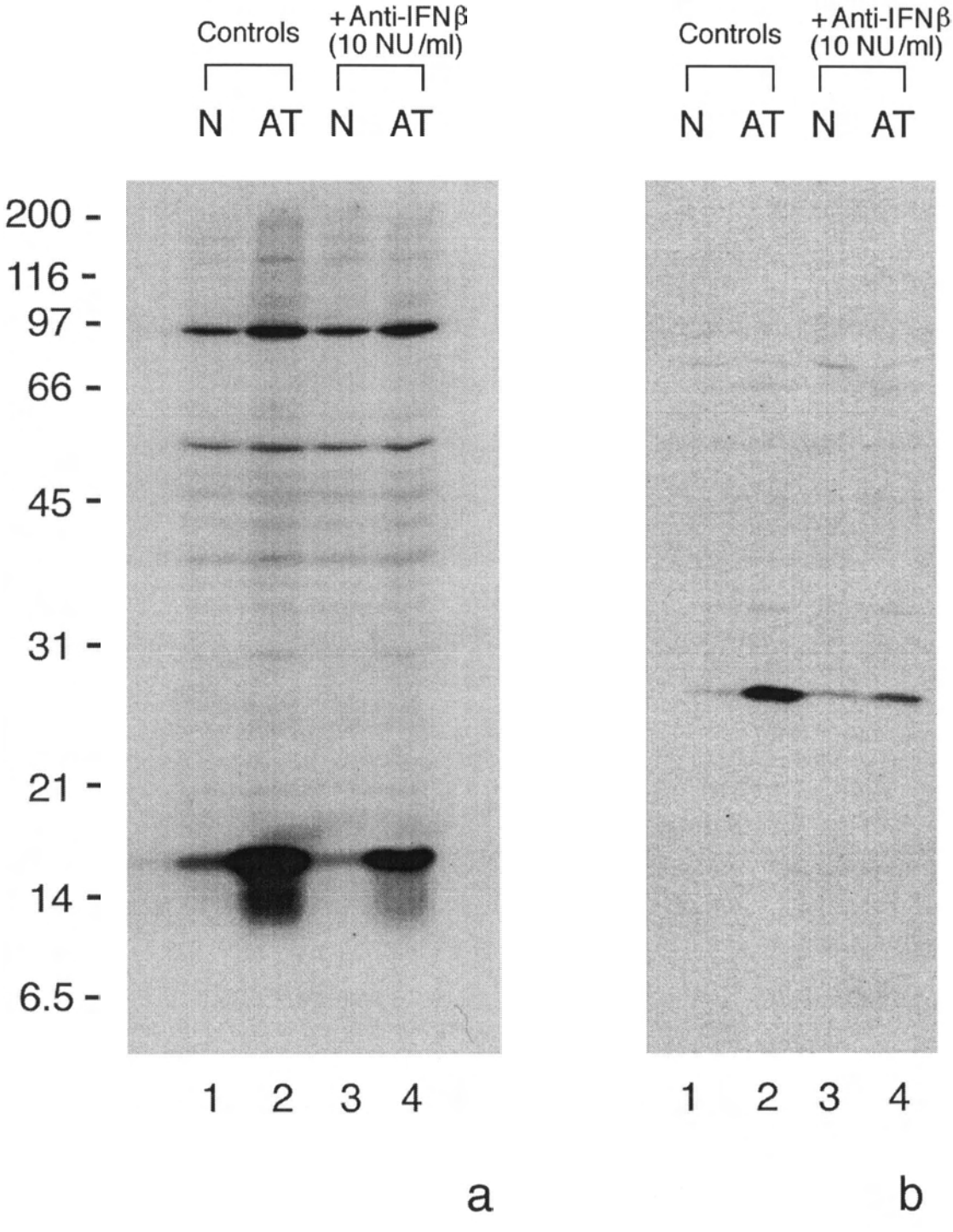
Controls
+Anti-IFNβ (10 NU/ml)
N AT N AT
200 -
116 -
97 -
66 -
45 -
31 -
21 -
14 -
6.5 -
1 2 3 4
a
Controls
+Anti-IFNβ (10 NU/ml)
N AT N AT
1 2 3 4
b

Figure 5.

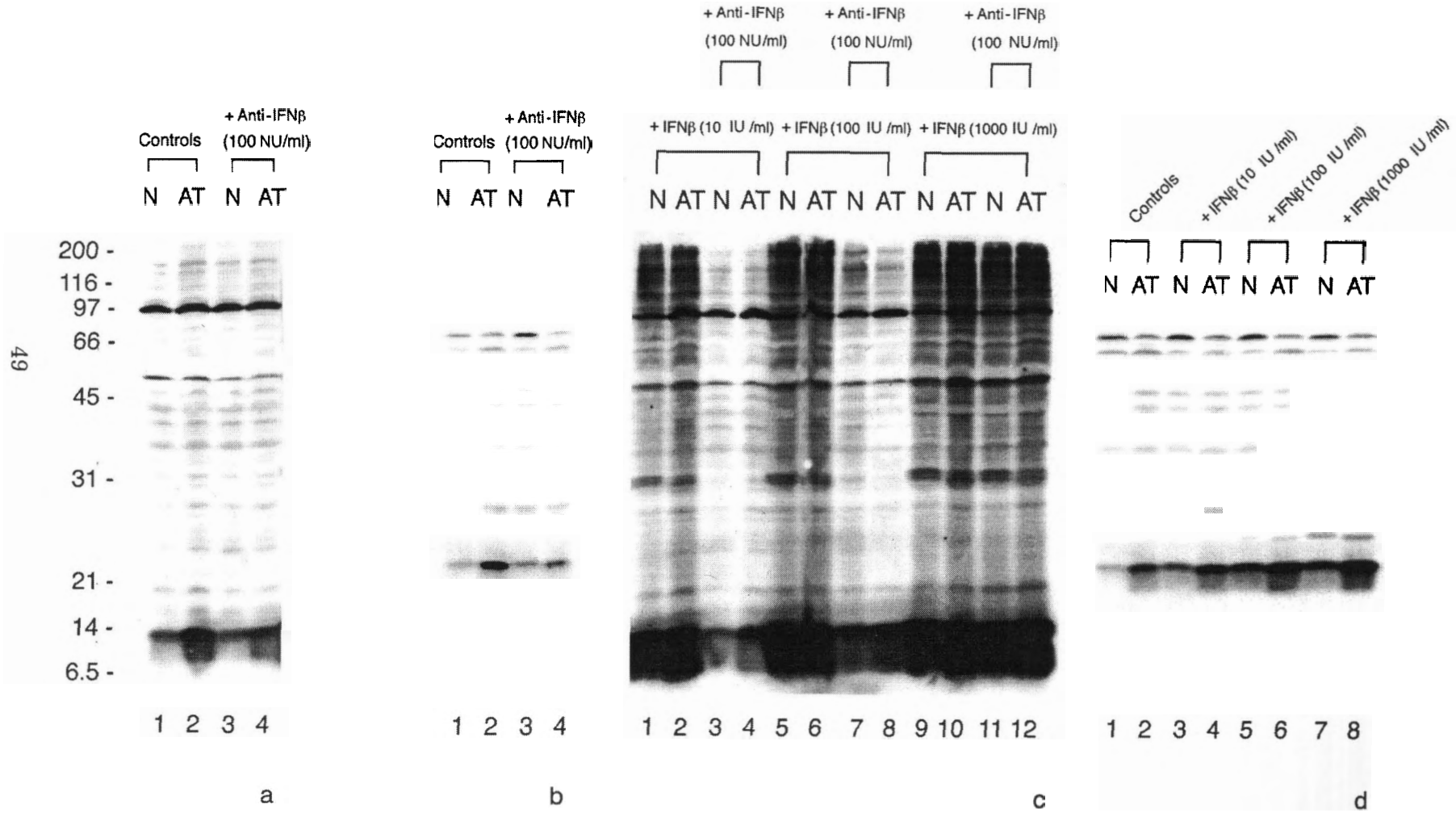
Controls
+ Anti-IFNβ (100 NU/ml)
N AT N AT
200 -
116 -
97 -
66 -
45 -
31 -
21 -
14 -
6.5 -
49
1 2 3 4
a
Controls
+ Anti-IFNβ (100 NU/ml)
N AT N AT
1 2 3 4
b
+ Anti-IFNβ (100 NU/ml)
+ Anti-IFNβ (100 NU/ml)
+ Anti-IFNβ (100 NU/ml)
+ IFNβ (10 IU /ml)
+ IFNβ (100 IU /ml)
+ IFNβ (1000 IU /ml)
N AT N AT N AT N AT N AT N AT
1 2 3 4 5 6 7 8 9 10 11 12
c
Controls
+ IFNβ (10 IU /ml)
+ IFNβ (100 IU /ml)
+ IFNβ (1000 IU /ml)
N AT N AT N AT N AT
1 2 3 4 5 6 7 8
d

Figure 6.

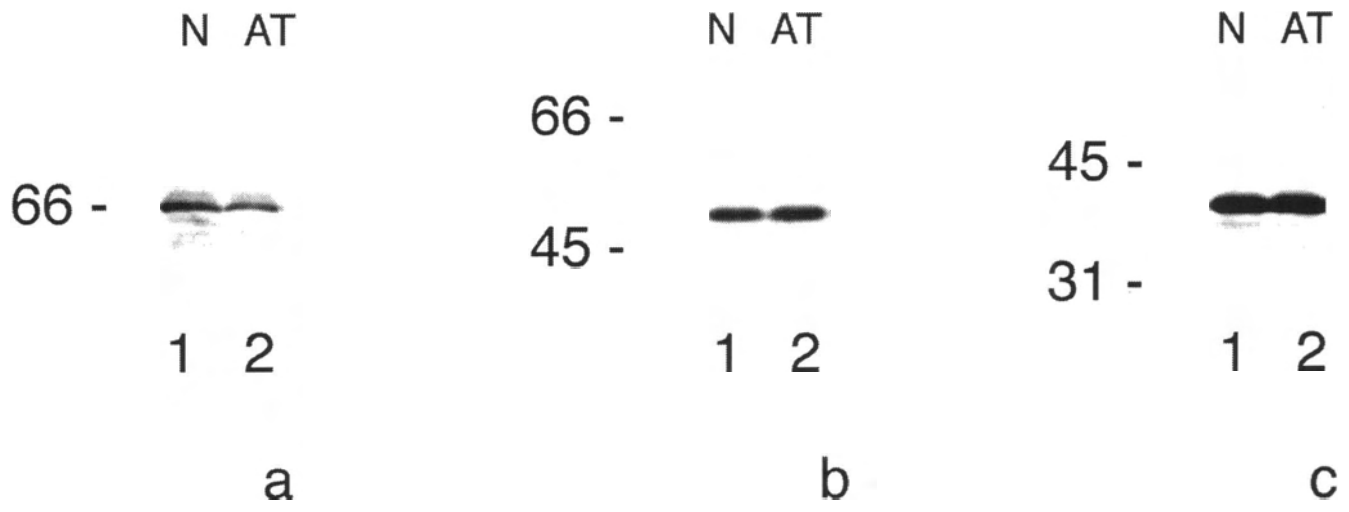

IMMUNOLOCALIZATION OF UCRP IN ATAXIA-TELANGIECTASIA CELLS

ABSTRACT

One of the most generalized phenomena among ataxia-telangiectasia (AT) cell lines is that they do not undergo the cell cycle arrest following ionizing radiation treatment typical of normal cells in the G1 and G2 phases of the cell cycle but, subsequently, experience a prolonged delay in G2/M. As certain yeast cell cycle mutants with post-irradiation defects similar to AT have been well characterized as ubiquitin conjugation mutants, the hypothesis tested in this study was that AT cells may display altered ubiquitin or ubiquitin cross-reactive protein (UCRP) kinetics. Using immunocytochemical techniques, we investigated the cellular localization of ubiquitin and of the interferon-inducible protein, UCRP, in two normal human fibroblast lines and in two human fibroblast lines obtained from AT patients. No differences in ubiquitin localization were observed between normal and AT cells. However, UCRP levels were consistently elevated in dividing and stationary AT cells as compared with normal cells. As reported previously, UCRP was found to be distributed in a cytoplasmic fibrous pattern closely resembling that for cytoskeletal proteins. Given our observation, we suggest that some critical element of UCRP regulation, which could have possible consequences for the cell cycle, may be affected in AT cells.

INTRODUCTION

Ataxia-telangiectasia (AT) is an autosomal recessive genetic disorder, which is characterized by loss of coordination and telangiectases, hypersensitivity to ionizing radiation, progressive neuronal degeneration, immunodeficiency and cancer proneness (1). One of the most generalized phenomena among cultured AT cell lines is that they do not undergo the inhibition of DNA synthesis following ionizing radiation treatment typical of normal cells (1,2). Usually, following ionizing irradiation treatment, cultured human cells block in G1-S and G2-M phase of the cycle in order to repair the DNA damage caused by the X-rays. However, in the case of AT, flow cytometric studies have consistently revealed that AT cells do not undergo an X-ray induced G1-S or G2-M delay, but subsequently experience a prolonged delay in G2/M (1,3,4). Interestingly, AT cells have also been reported to display altered cellular morphology due to a more abundant and well defined actin microfilament array than normal cells (5).

A yeast cell cycle mutant with a post-irradiation defect similar to AT has been well characterized. RAD6 mutants of S. cerevisiae are extremely sensitive to DNA damage caused by ultraviolet light, X-rays and chemical mutagens, as they are totally deficient in repairing mutagenesis induced by these agents. The RAD6 gene encodes a ubiquitin-conjugating enzyme of the E2 family (6). A homologous gene, the yeast CDC34 gene encodes a related ubiquitin-conjugating E2 isozyme that is required for the transition of cells from G1 to S phase in the cell cycle (7). Therefore, we postulated that AT cells may possess altered ubiquitin or ubiquitin cross-reactive protein (UCRP) kinetics which could result in perturbations of the cell cycle.

Previous Western blotting studies have revealed that UCRP, but not ubiquitin, levels are elevated in AT cells. Using an immunocytochemical approach, we decided to investigate possible differences in cellular localization of UCRP between dividing and stationary, AT and normal fibroblasts. Although no major differences in ubiquitin localization between dividing and stationary AT and normal cells appear to exist, we found that dividing and stationary AT fibroblasts consistently stained intensely for UCRP. In contrast, UCRP staining was consistently faint in stationary normal fibroblasts, while it was variable in dividing normal fibroblasts. Since UCRP has been found to associate with certain cytoskeletal proteins which may be involved in cell cycle regulation, the observations presented in this paper may be relevant to differences in cell cycle that exist between AT and normal cells (8).

MATERIALS AND METHODS

Chemicals. Bovine serum albumin, Tris, and ρ-phenylenediamine were purchased from Sigma. Glycine and diethyl ether were from BDH.

Antibodies. Rabbit anti-ubiquitin and anti-UCRP polyclonal antibodies were generated against SDS-denatured ubiquitin and recombinant mature human UCRP, respectively, and then they were affinity purified, as previously described (9,10). FITC-conjugated goat anti-rabbit IgG antibodies were bought from Sigma.

Cell Lines and Culture. Strains of normal (5757 and 8333) and AT (1588 and 2052) non-transformed human fibroblasts were obtained from the Coriell Institute (Camden, NJ). Fibroblast cultures were grown in Dulbecco's modified Eagles media (D-MEM, Flow, McLean, VA) supplemented with 15% heat-inactivated fetal calf serum (FCS, Gibco, Grand Island, NY), penicillin (100 units/ml) and streptomycin (100

μg/ml). All stock cultures were maintained in 75-cm^2 culture flasks at 37°C in incubators with a 5% CO_2/95% air atmosphere.

Immunofluorescence. Cultures of 5757, 1588, 8333 and 2052 primary fibroblasts were grown to log phase or stationary phase on glass coverslips. The cells were rinsed twice with phosphate-buffered saline and fixed successively with 70% ethanol for 15 min, 50% ethanol/50% ether for 30 min, 70% ethanol for 3 min, 50% ethanol for 15 min, and H_2O for 15 min. Fixed cells were then rinsed five times in PBS. The samples were blocked by incubating them in Blocking Solution [50 mM Tris-Cl (pH 7.6), 150 mM NaCl, and 25 mg/ml BSA] for 30 min to eliminate non-specific binding. The coverslips were incubated with anti-ubiquitin or anti-UCRP antibodies (10 μg/ml) diluted in Blocking Solution at room temperature for 1 hour. This was followed by three rinses of 10 min each with Tris-saline. Next, the cells were incubated for 1 hour at room temperature with FITC-conjugated goat anti-rabbit antibody and the coverslips were rinsed three times with Tris-saline. The coverslips were inverted and mounted onto glass slides using a glycine buffer containing the antiquenching agent, ρ-phenylenediamine (0.1%). The slides were viewed under an Olympus fluorescence microscope using a blue FITC filter with absorbance maximum at 495 nm.

RESULTS

Immunocytochemical Localization of Ubiquitin in Log Phase Cells. In order to test whether ubiquitin levels are similar in normal and AT cells in logarithmic growth phase, two normal (5757,8333) and two AT (1588,2052) fibroblast lines were grown on glass coverslips to log phase and were fixed. The fixed cells were incubated with

affinity purified anti-ubiquitin antibody specific for the conjugated form of ubiquitin at a concentration of 10 μg/ml and incubated with 10 μg/ml of FITC-conjugated goat anti-rabbit antibody. The intracellular distribution of ubiquitin was determined using an Olympus fluorescent microscope. In both normal cell lines (Fig. 1A & C), nuclear and cytoplasmic staining was observed, demonstrating the existence of conjugated ubiquitin in dividing normal fibroblasts. In the two AT cell lines (Fig.1B & D), the nuclear and cytoplasmic staining was comparable to that observed in the normal cell lines demonstrating the existence of apparently normal pools of conjugated ubiquitin in dividing AT fibroblasts. The background fluorescence in the non-immune controls was negligible (Fig.5). When viewed under a light microscope, the density of the control cells was equivalent to that of the cells incubated with the primary antibody.

Immunocytochemical Localization of Ubiquitin in Stationary Cells. In order to test whether ubiquitin levels are similar in quiescent normal and AT cells, the same two normal and AT fibroblast lines were grown on glass coverslips to confluency and were treated as described above. In both normal cell lines (Fig. 2A & C), some nuclear and cytoplasmic staining was observed, demonstrating the existence of conjugated ubiquitin in stationary normal fibroblasts. In the two AT cell lines (Fig.2B & D), the nuclear and cytoplasmic staining was comparable to that observed in the normal cell lines demonstrating the existence of apparently normal pools of conjugated ubiquitin in stationary AT fibroblasts. The background fluorescence in the non-immune controls was negligible (Fig.6). When viewed under a light microscope, the density of the control cells was equivalent to that of the cells incubated with the primary antibody.

Immunocytochemical Localization of UCRP in Log Phase Cells. In order to test whether UCRP levels are similar in dividing normal and AT cells, the same two normal

and AT fibroblast lines were grown on glass coverslips to log phase and were fixed. The fixed cells were incubated with affinity purified anti-UCRP antibody that recognizes both conjugated and unconjugated forms of UCRP at a concentration of 10 μg/ml and incubated with 10 μg/ml of FITC-conjugated goat anti-rabbit antibody. In the past, immunofluorescence studies have revealed that UCRP tends to have a cytoplasmic fibrous distribution closely resembling that for cytoskeletal proteins with a perinuclear pattern that becomes more punctate toward the cell periphery (10). In fact, UCRP conjugates have been found to be distributed along intermediate filaments of the keratin and vimentin variety in human cells (10). In one of the normal cell lines (Fig.3A), almost no staining was visible demonstrating very low levels of UCRP, while in the other normal cell line some staining with a perinuclear pattern and a cytoplasmic fibrous distribution was observed (Fig.3C) demonstrating the existence of UCRP. Thus, this difference in intensity of staining between the 8333 cell line and the 5757 cell line suggests that there is some variability in the levels of UCRP in normal dividing cells, perhaps according to stage of the cell cycle. However, in both AT cell lines (Fig.3B & D), staining with a characteristic perinuclear pattern and a cytoplasmic fibrous distribution was observed demonstrating the existence of UCRP pools in dividing AT fibroblasts. The latter result suggests that perhaps there is not much variation in the UCRP levels of dividing AT cells. Based on previous data, the UCRP in the normal and AT cells may be associated with intermediate filaments of the cytoskeletal network. The background fluorescence in the non-immune controls was negligible (Fig.5). When viewed under a light microscope, the density of the control cells was equivalent to that of the cells incubated with the primary antibody.

Immunocytochemical Localization of UCRP in Stationary Cells. In order to test whether UCRP levels are similar in quiescent normal and AT cells, the same two

normal and AT fibroblast lines were grown on glass coverslips to confluency and were treated as described above. In both normal cell lines (Fig.4A & C), very weak cytoplasmic staining was observed, demonstrating the existence of very low levels of UCRP in stationary normal fibroblasts. However, in the two AT cell lines (Fig.4B & D), intense cytoplasmic staining with a fibrous distribution was observed as compared to the normal cell lines demonstrating the existence of high levels of UCRP in stationary AT fibroblasts. The background fluorescence in the non-immune controls was negligible (Fig.6). When viewed under a light microscope, the density of the control cells was equivalent to that of the cells incubated with the primary antibody.

DISCUSSION

From the results obtained using immunochemical techniques, there are no apparent differences in ubiquitin levels between log and stationary phase normal and AT cells. However, UCRP levels appear to be elevated in stationary AT cells as compared with stationary normal cells in which UCRP is barely detectible. In addition, it appears that UCRP levels are variable between different cultures of dividing normal cells, while they are not as variable between different cultures of dividing AT cells. Moreover, variations in UCRP pools appear to be growth phase dependent since UCRP, when present, is more abundant in dividing than in stationary normal cells. The difference in UCRP levels between the two different cultures of dividing normal fibroblasts may be explained by a difference in rate of cell division such that one culture may have a higher percentage of cells in G1, S, or G2 phase than the other culture at any given time. In contrast, in AT cells, UCRP

levels do not appear to be as variable between different cultures of stationary and dividing cells suggesting a difference in the dynamics of UCRP pools between AT and normal cells. Cell synchronization coupled with flow cytometry would be very useful for comparing variations in UCRP according to each stage of the cell cycle between normal and AT cells.

The results presented above indicate that UCRP is overexpressed in dividing and stationary AT cells. Interestingly, a previous immunocytochemical study revealed that UCRP levels are constitutively present in human lung carcinoma cells (10). UCRP is a 15 kDa protein that is highly homologous in its sequence to ubiquitin, one of the most highly conserved eukaryotic proteins. Ubiquitin is involved in tagging cellular proteins for destruction via an energy-dependent conjugation process. As the crucial role of ubiquitin in the programmed destruction of specific proteins such as cyclins during the cell cycle has been generally acknowledged, changes in ubiquitin conjugation kinetics can have a profound impact on the cell cycle (11,12). UCRP has also been found conjugated to many other proteins including proteins that bind to intermediate filaments of the cytoskeleton such as cytokeratins and vimentin (8,13). However, the biochemical significance of this process is still unclear.

The role of cytoskeletal proteins in the cell cycle, particularly during mitosis, is extensive. Immunofluorescence studies have revealed that proteasomes colocalize with intermediate filaments of the cytokeratin type during G2 and around M phase of the cell cycle (14). As proteasomes have been implicated in cell cycle regulation via specific protein degradation, this association of proteasomes with cytokeratins may indicate a timely degradation event during the cell cycle. Furthermore, the intermediate filament-associated protein (IFAP), IFAP 300, has been shown to be a physiological substrate of the $p34^{cdc2}$ kinase which coordinates the mitotic

reorganization of the vimentin intermediate filament network mediated by IFAP 300 as a result (15). Efficient exit from mitosis also occurs only under conditions where $p34^{cdc2}$ kinase remains associated with centrosomal microtubules, suggesting that normal mitotic exit may be regulated by the microtubule assembly state (16). It has been demonstrated in cycling cells that eukaryotic elongation factor 2 (eEF-2) is located near the nucleus in the endoplasm. Following the transition from proliferation to G0 phase of the cell cycle, eEF-2 becomes redistributed mainly along the intermediate filaments and/or microtubules. Reversion of the cells to a proliferative state is accompanied by rearrangement of the actin cytoskeleton resulting in the original pattern of eEF-2 distribution (17). So, it appears that the different cytoskeletal elements in eukaryotic cells can be involved in organizing the protein-synthesizing machinery according to phase of the cell cycle. Thus, given the above, it seems plausible that the regulated induction of UCRP could have possible consequences for the cell cycle by increasing its association with specific proteins that produce changes in cytoskeletal structure.

The gene for ATM has been recently identified and its product may function in signal transduction (18). The pathway for UCRP regulation may be affected by this gene resulting in the constitutive elevation of UCRP which we have observed in AT cells. UCRP is one of a number of proteins that are induced in cells following interferon α and ß treatments (13). Interferons are responsible for producing a wide range of biological effects including virus inhibition, slowing of cell proliferation, immunomodulation, and alterations in differentiation. Usually, the induction of interferon-inducible genes is transient lasting only 6-8 hours even in the continued presence of the inducer (19). However, previous Western blotting studies have revealed constitutive activation of the interferon ß gene resulting in continuous induction of free UCRP in AT cells with no corresponding increase in UCRP

conjugation (20). Therefore, using flow cytometry, it would be interesting to determine if any differences in UCRP induction and conjugation occur between synchronized normal and AT cells following X-ray-induced DNA damage. The constitutive elevation of UCRP in AT cells may be linked to the abnormal cell cycle kinetics observed in AT cells following ionizing radiation treatment, as constitutive activation of the growth inhibitory interferon ß gene may be indicative of a faulty DNA damage response pathway in AT cells. This DNA damage response pathway may normally stimulate UCRP conjugation to proteins that determine changes in cytoskeletal structure according to phase of the cell cycle.

REFERENCES

1. McKinnon, P.J. Ataxia-telangiectasia: an inherited disorder of ionizing-radiation sensitivity in man. Hum. Genet., 75: 197-208, 1987.
2. Taylor, A.M.R., Byrd, P.J., McConville, C.M., and Thacker, S. Genetic and cellular features of ataxia telangiectasia. Int. J. Radiat. Biol., 65 (1): 65-70, 1994.
3. Beamish, H., Khanna, K., Lavin, M.F., Ionizing radiation and cell cycle progression in ataxia telangiectasia. Radiat. Res., 138: S130-S133, 1994.
4. Beamish, H., and Lavin, M.F., Radiosensitivity in ataxia telangiectasia: anomalies in radiation-induced cell cycle delay. Int. J. Radiat. Biol., 65(2): 175-184, 1994.
5. McKinnon, P.J., and Burgoyne, L.A. Altered cellular morphology and microfilament array in ataxia-telangiectasia fibroblasts. Eur. J. Cell Biol., 39: 161-166, 1985.
6. Jentsch, S., McGrath, J.P., and Varshavsky, A. The yeast DNA repair gene RAD6 encodes a ubiquitin-conjugating enzyme. Nature, 329: 131-134, 1987.
7. Goebl, M.G., Yochem, J., Jentsch, S., McGrath, J.P., Varshavsky, A., and Byers, B. The yeast cell cycle gene CDC34 encodes a ubiquitin-conjugating enzyme. Science, 241: 1331-1335, 1988.
8. Loeb, K.R. and Haas, A.L. Cytoskeletal distribution of UCRP conjugates. Mol. & Cell. Biol., 14(12): 8408-8419, 1994.
9. Haas, A.L., Ahrens, P., Bright, P.M., and Ankel, H. Interferon induces a 15-kilodalton protein exhibiting marked homology to ubiquitin. J. Biol. Chem., 262(23): 11315-11323, 1987.
10. Haas, A.L. and Bright, P.M. The immunochemical detection and quantitation of intracellular ubiquitin-protein conjugates. J. Biol. Chem., 260(23): 12464-12473, 1985.
11. Mayer, R.J. and Doherty, F.J. Ubiquitin. Essays - Biochem., 27: 37-48,

1992.

12. Pines, J. Ubiquitin with everything. Nature, 371: 742-743, 1994

13. Loeb, K.R. and Haas, A.L. The interferon-inducible 15-kDa ubiquitin homolog conjugates to intracellular proteins. J. Biol. Chem., 267(11): 7806-7813, 1992.

14. Palmer, A., Mason, G.G.F., Paramio, J.M., Knecht, E. and Rivett, A.J. Changes in proteasome localization during the cell cycle. Eur. J. Cell Biol., 64: 163-175, 1994.

15. Skalli, O., Chou, Y.-H. and Goldman, R.D. Cell cycle-dependent changes in the organization of an intermediate filament-associated protein: correlation with phosphorylation by $p34^{cdc2}$. Proc. Natl. Acad. Sci. USA, 89: 11959-11963, 1992.

16. Andreassen, P.R. and Margolis, R.L. Microtubule dependency of $p34^{cdc2}$ inactivation and mitotic exit in mammalian cells. J. Cell. Biol., 127 (3): 789-802, 1994.

17. Shestakova, E.A., Motuz, L.P. and Gavrilova, L.P. Co-localization of components of the protein-synthesizing machinery with the cytoskeleton in G_0-arrested cells. Cell Biol. Int., 17(4): 417-424, 1993.

18. Savitsky, K., Bar-Shira, A., Shlomit, G., Rotman, G., Ziv, Y., Vanagaite, L., Tagle, D.A., Smith, S., Uziel, T., Sfez, S., Askenazi, M., Pecker, I., Frydman, M., Harnik, R., Patanjali, S.R., Simmons, A., Clines, G.A., Sartiel, A., Gatti, R.A., Chessa, L., Sanal, O., Lavin, M.F., Jaspers, N.G.J., Taylor, M.R., Arlett, C.F., Miki, T., Weissman, S.W Lovett, M., Collins, F.S. and Shiloh, Y. A single ataxia telangiectasia gene with a product similar to PI-3 kinase. Science, 268: 1749-1753, 1995.

19. Akai, H. and Larner, A.C. Phorbol ester-mediated down-regulation of an interferon-inducible gene. J. Biol. Chem., 264(6): 3252-3255, 1989.

20. Siddoo-Atwal, C., Haas, A.L., and Rosin, M.P. Elevation of interferon ß-inducible proteins in ataxia telangiectasia cells. Cancer Res., 56: 443-447, 1996.

FIGURE LEGENDS

Figure 1. Immunocytochemical Detection of Ubiquitin in Dividing Normal and AT Fibroblasts. Normal (5757,8333) and AT (1588,2052) fibroblast cultures were grown on glass coverslips to log phase, rinsed with PBS twice and fixed. The fixed cells were stained with affinity purified anti-ubiquitin (10 μg/ml) and incubated with FITC-conjugated (10 μg/ml) goat anti-rabbit antibodies. **A.** normal (5757) fibroblasts **B.** AT (1588) fibroblasts **C.** normal (8333) fibroblasts **D.** AT (2052) fibroblasts

Figure 2. Immunocytochemical Detection of Ubiquitin in Stationary Normal and AT Fibroblasts. Normal (5757,8333) and AT (1588,2052) fibroblast cultures were grown on glass coverslips to confluency, rinsed with PBS twice and fixed. The fixed cells were stained with affinity purified anti-ubiquitin (10 μg/ml) and incubated with FITC-conjugated (10 μg/ml) goat anti-rabbit antibodies. **A.** normal (5757) fibroblasts **B.** AT (1588) fibroblasts **C.** normal (8333) fibroblasts **D.** AT (2052) fibroblasts

Figure 3. Immunocytochemical Detection of UCRP in Dividing Normal and AT Fibroblasts. Normal (5757,8333) and AT (1588,2052) fibroblast cultures were grown on glass coverslips to log phase, rinsed with PBS twice and fixed. The fixed cells were stained with affinity purified anti-UCRP (10 μg/ml) and incubated with FITC-conjugated (10 μg/ml) goat anti-rabbit antibodies. **A.** normal (5757) fibroblasts **B.** AT (1588) fibroblasts **C.** normal (8333) fibroblasts **D.** AT (2052) fibroblasts

Figure 4. Immunocytochemical Detection of UCRP in Stationary Normal and AT Fibroblasts. Normal (5757,8333) and AT (1588,2052) fibroblast cultures were grown on glass coverslips to confluency, rinsed with PBS twice and fixed. The fixed cells were stained with affinity purified anti-UCRP (10 μg/ml) and incubated with FITC-conjugated (10 μg/ml) goat anti-rabbit antibodies. **A.** normal (5757) fibroblasts **B.** AT (1588) fibroblasts **C.** normal (8333) fibroblasts **D.** AT (2052) fibroblasts

Figure 5. Log Phase Controls. Normal (5757,8333) and AT (1588,2052) fibroblast cultures were grown on glass coverslips to log phase, rinsed with PBS twice and fixed. The fixed cells were incubated with FITC-conjugated (10 μg/ml) goat anti-rabbit antibodies. **A.** normal (5757) fibroblasts **B.** AT (1588) fibroblasts **C.** normal (8333) fibroblasts **D.** AT (2052) fibroblasts

Figure 6. Stationary Phase Controls. Normal (5757,8333) and AT (1588,2052) fibroblast cultures were grown on glass coverslips to confluency, rinsed with PBS twice and fixed. The fixed cells were incubated with FITC-conjugated (10 μg/ml) goat anti-rabbit antibodies. **A.** normal (5757) fibroblasts **B.** AT (1588) fibroblasts **C.** normal (8333) fibroblasts **D.** AT (2052) fibroblasts

Figure 1.

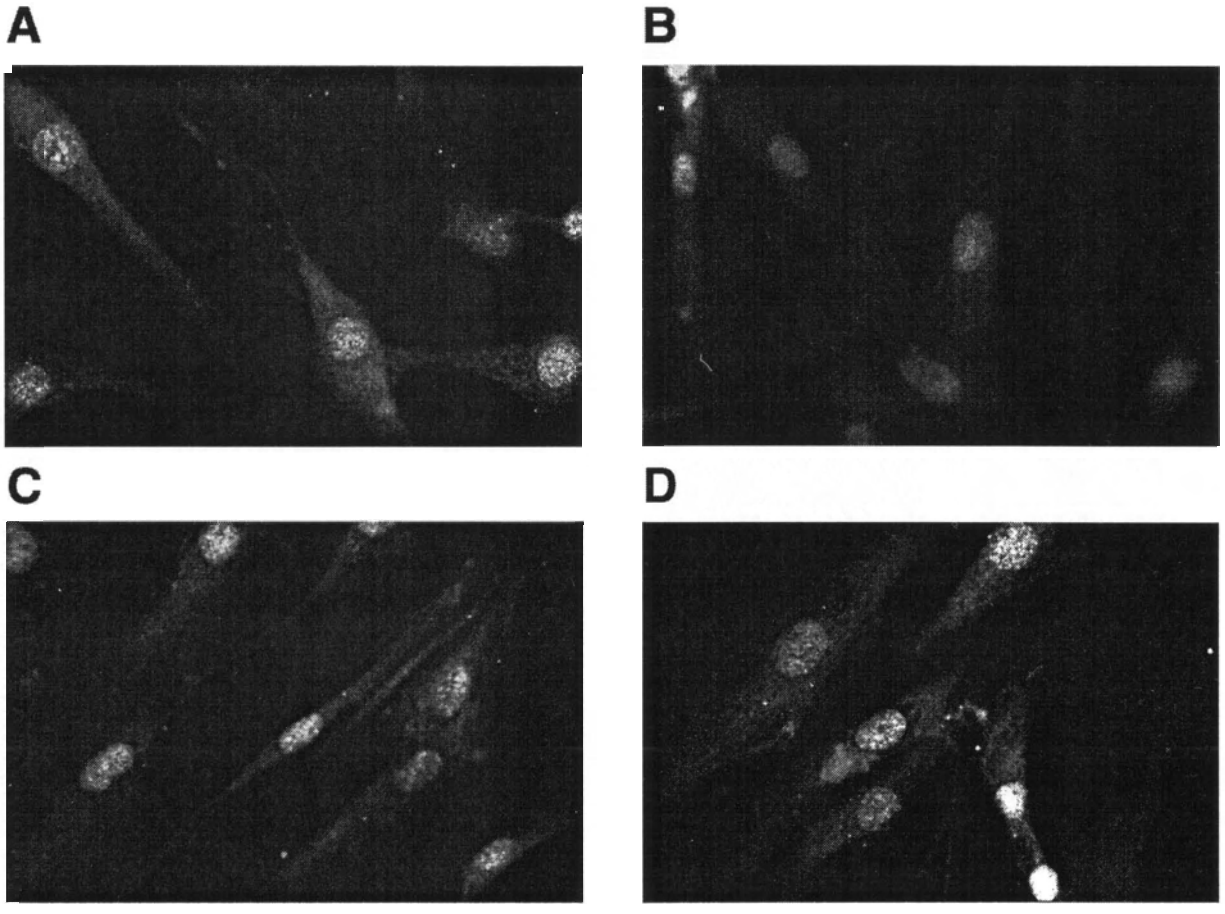

Figure 2.

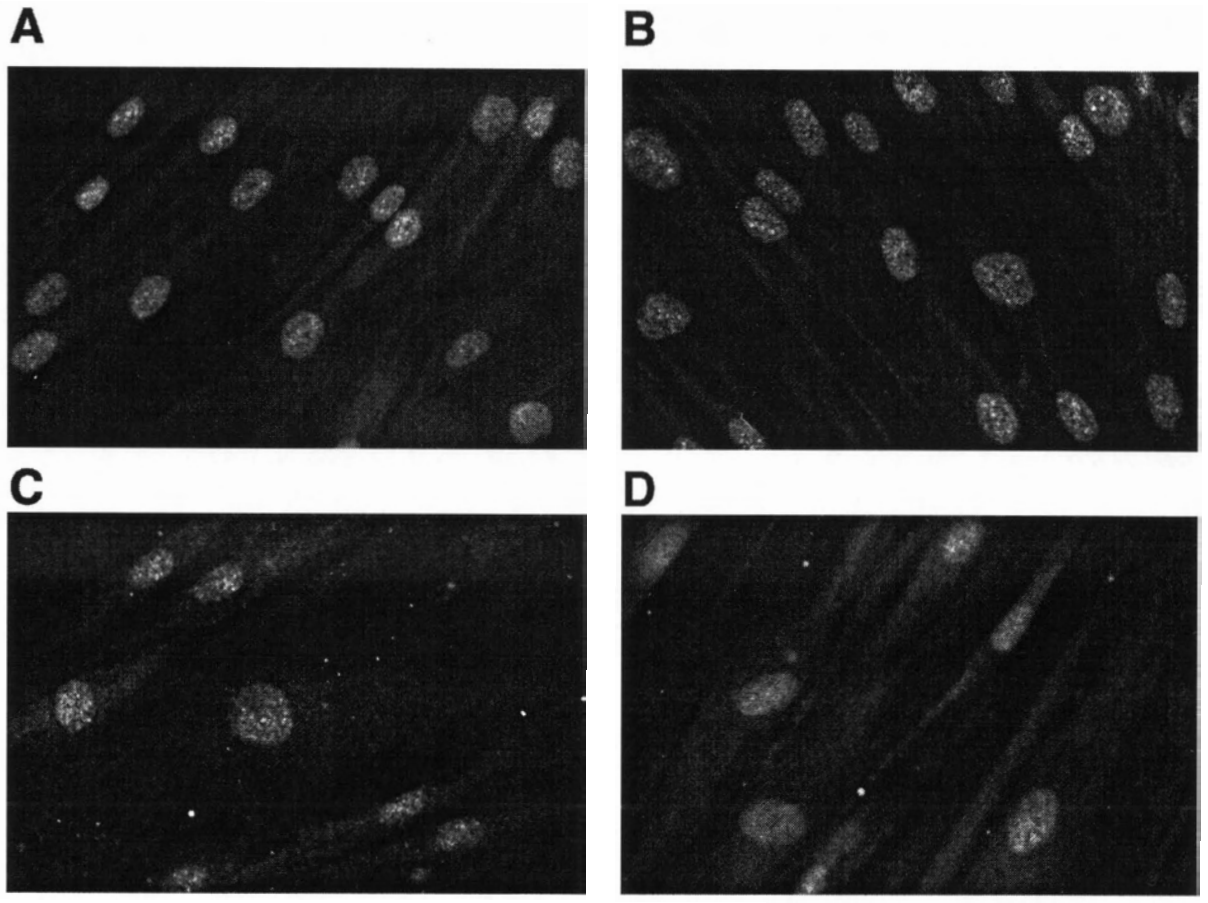

Figure 3.

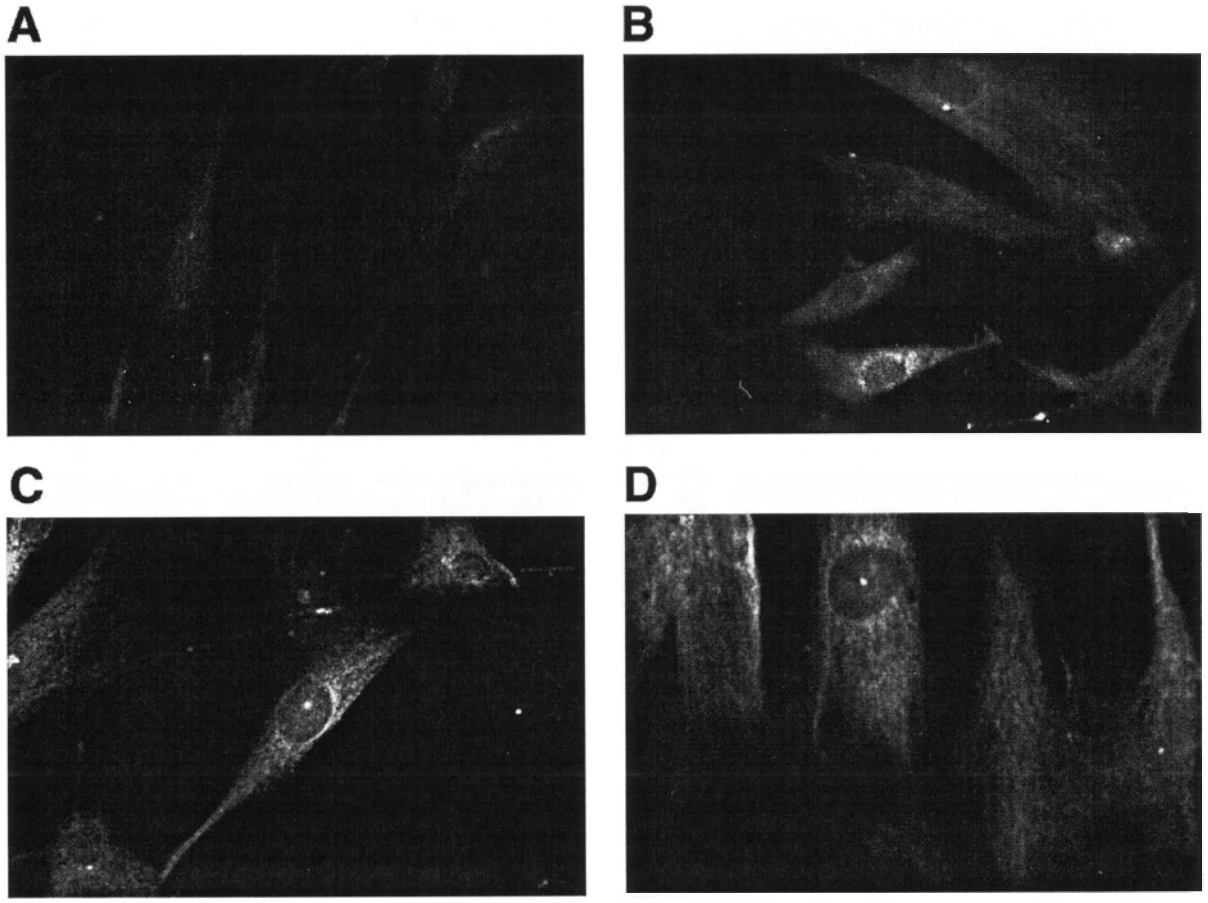

Figure 4.

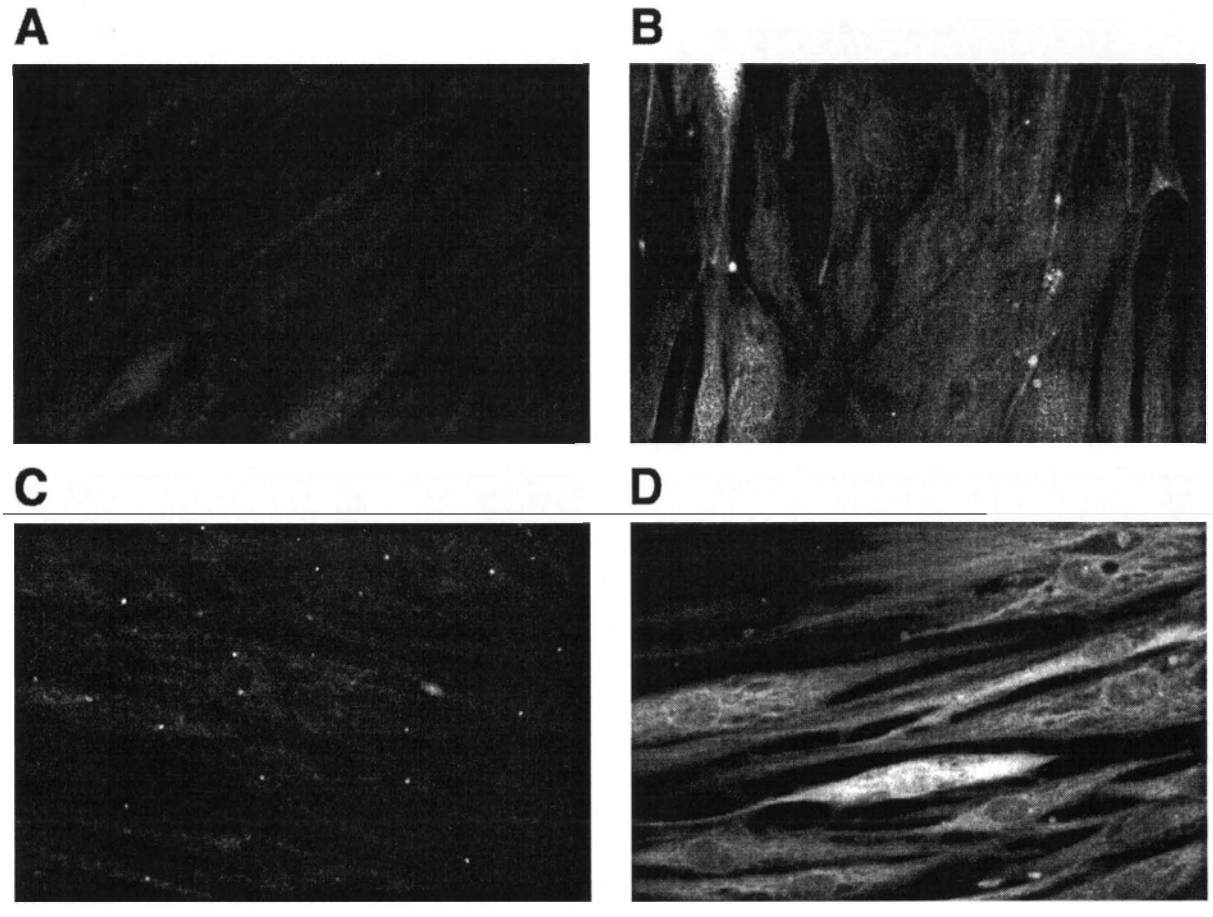

Figure 5.

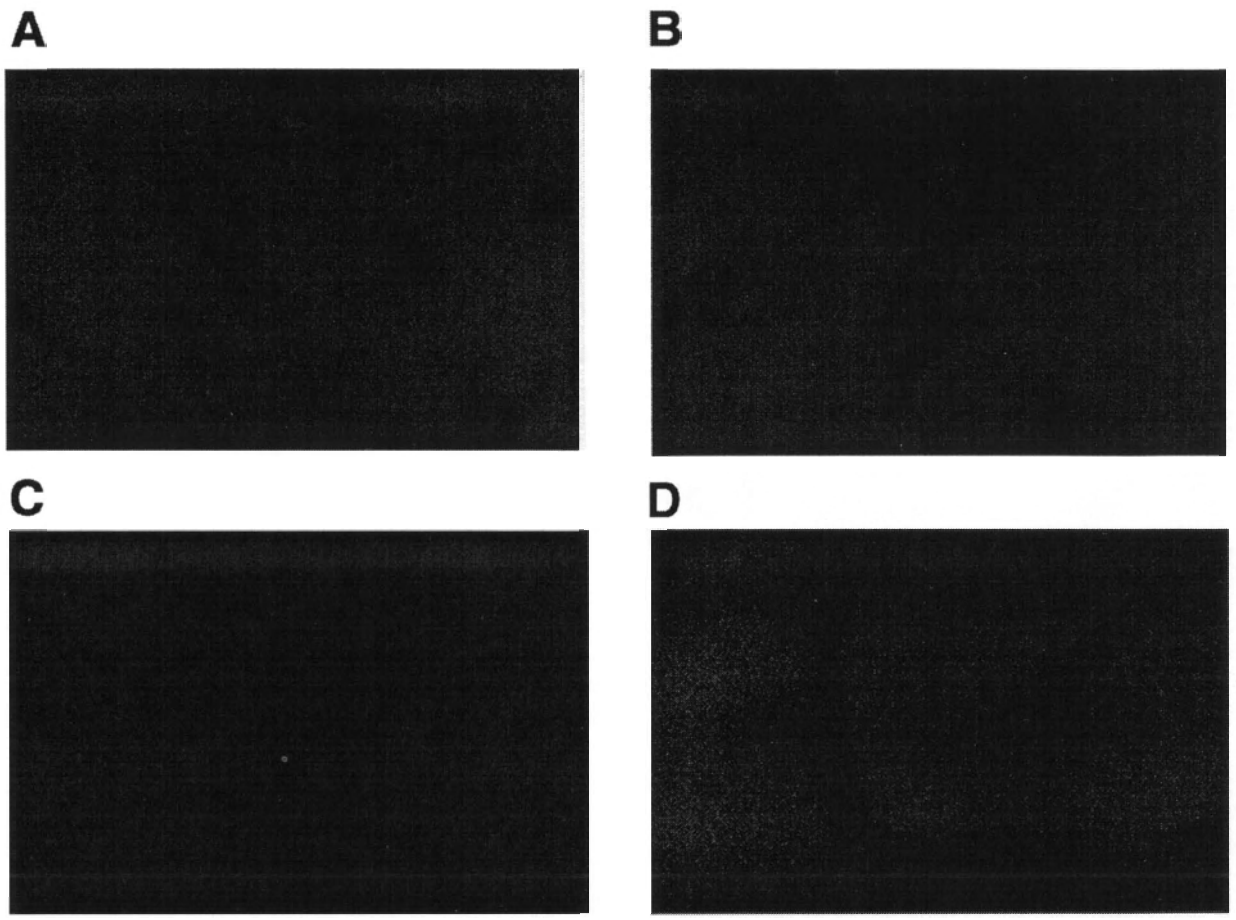

Figure 6.

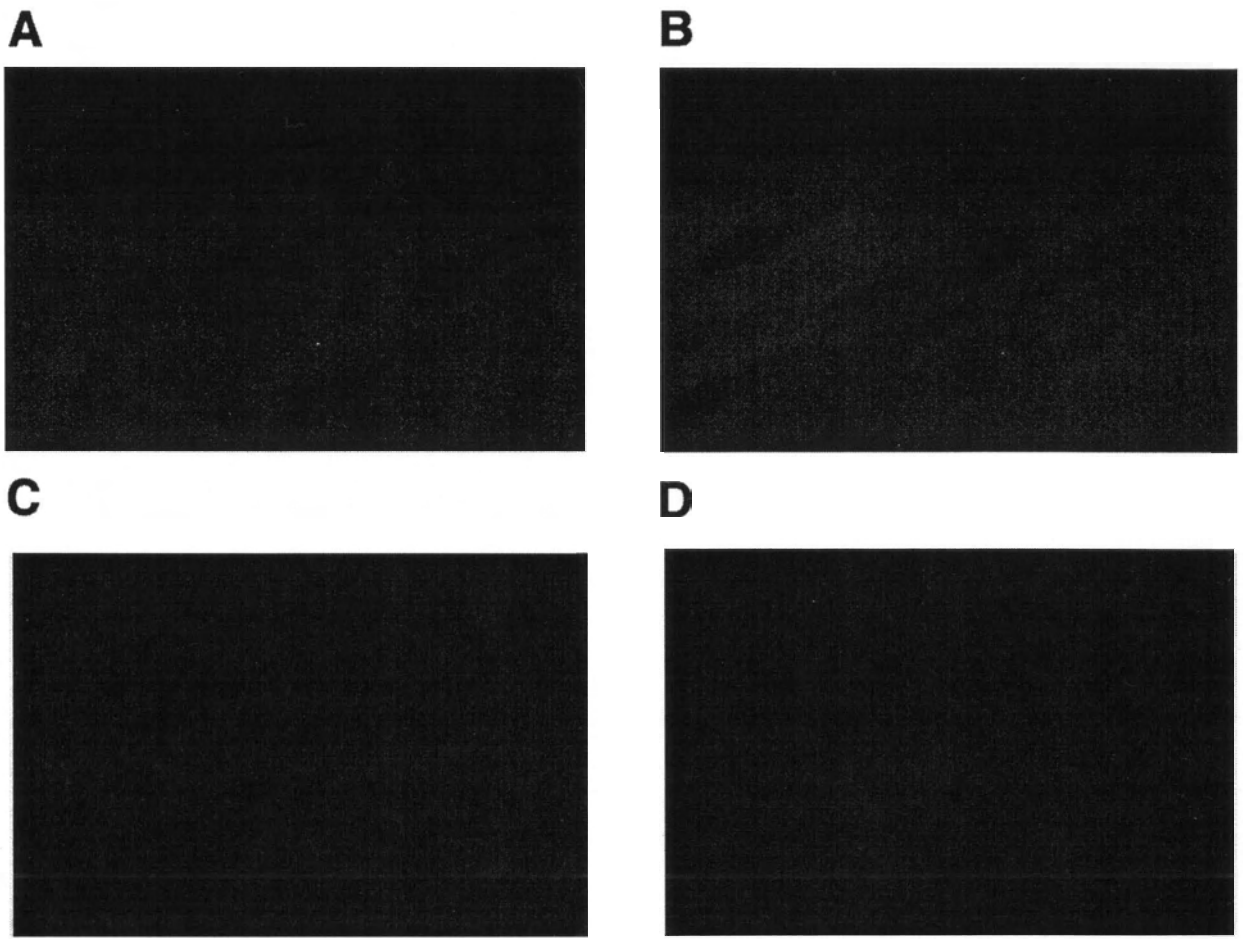

A PRELIMINARY STUDY OF UCRP LEVELS IN HUMAN LUNG AND BLADDER CANCERS

ABSTRACT

Constitutive activation of the interferon ß gene has been previously shown to cause the continuous induction of UCRP observed in AT cells, probably as a result of a defect in the NF-κB activation pathway. As one of the main clinical features of AT is cancer proneness, investigating the distribution of UCRP in cancer cells may be significant. In this preliminary study, we report elevated levels of ubiquitin cross-reactive protein (UCRP) in human lung and bladder tumour tissue sections using immunohistochemical techniques. The abnormally high expression of UCRP in two different human ataxia-telangiectasia (AT) fibroblast strains was compared to that in the cancerous tissues. It is possible that the elevation of UCRP in cancer cells may also result from constitutive activation of the interferon ß gene. Interferons are responsible for producing a wide range of biological effects including virus inhibition, slowing of cell proliferation, immunomodulation and alterations in differentiation. This group of molecules retards the growth and proliferation of cells by prolonging the cell cycle and inhibiting the expression of certain proto-oncogenes. Thus, a dysregulation of the activation pathway for interferon ß may represent a fundamental change in cell metabolism in the early stages of carcinogenesis.

INTRODUCTION

Ubiquitin, a protein consisting of 76 amino acids, is one of the most highly conserved proteins from yeast to humans (1). Together, proteasomes and ubiquitin comprise the ATP-dependent, nonlysosomal proteolytic pathway in eukaryotic cells. Ubiquitin is responsible for tagging cellular proteins for destruction via an energy-dependent conjugation pathway, while the proteolytic complexes known as proteasomes catalyze the actual breakdown of the ubiquitinated proteins (2,3). Ubiquitin has been found to be involved in a wide range of cellular functions including DNA repair, cell cycle progression, modification of polypeptide receptors and biogenesis of ribosomes (4,5,6,7). The fact that certain yeast cell cycle mutants, such as RAD6 and CDC34, encode mutant ubiquitin conjugation enzymes supports a role for ubiquitin in cell proliferation (4,5). Furthermore, various proteins including c-myc, c-fos, and p53 that are involved in cell cycle regulation have been shown to be degraded by ubiquitin-mediated proteolysis (8,9). Moreover, the crucial role of ubiquitin in the programmed destruction of specific proteins such as cyclins during the cell cycle has been generally acknowledged (10). An elevation of both proteasomes and ubiquitin has been reported in human renal cancer cells (11). Proteasome expression has also been found to be unusually high in human leukemic cells (12).

UCRP is a 15 kDa protein that is highly homologous in its sequence to ubiquitin and is one of a number of proteins that are induced in cells following interferon α and ß treatments (13). Interferons produce a wide range of biological effects, most notably the slowing of cell proliferation (14). They may also be involved in producing a coordinate cell cycle arrest with p53 (15). Like ubiquitin, UCRP has been found to be conjugated to many other proteins including those proteins which associate with certain cytoskeletal elements (16,17); however the

biochemical function of UCRP conjugation is currently unknown. Nevertheless, the role of cytoskeletal proteins in the cell cycle, particularly during mitosis, is extensive (18) and it is possible that UCRP may carry out an opposite function to ubiquitin in cell division, for example, arresting it simply by associating with regulatory proteins.

Ataxia-telangiectasia (AT) is a multi-faceted autosomal recessive genetic disorder that is characterized by loss of coordination and telangiectases, hypersensitivity to ionizing radiation, progressive neuronal degeneration, immunodeficiency and a predisposition to cancer (19). One of the most generalized phenomenon among cultured AT cell lines is that they do not undergo the inhibition of DNA synthesis following ionizing radiation to repair their DNA damage as do normal cells and, therefore, resemble a well characterized yeast cell cycle mutant (20). RAD6 mutants of S. cerevisiae are extremely sensitive to DNA damage caused by ultraviolet light, X-rays and chemical mutagens, as they are totally deficient in repairing genotoxic damage induced by these agents. The RAD6 gene encodes a ubiquitin-conjugating enzyme of the E2 family (4). Therefore, it seems possible that a mutation affecting UCRP metabolism could also have a profound effect on cell cycle kinetics.

Previous studies have revealed that UCRP levels, but not ubiquitin levels, are elevated in AT cells compared with normal cells due to a dysregulation of the interferon ß activation pathway (21). In the present study, to determine whether elevated UCRP levels are present in tumour cells, we used immunohistochemistry to examine the expression of UCRP in various human tumours. As observed in AT fibroblasts, using this technique, we showed that UCRP levels are also elevated in lung and bladder tumour tissues when compared with normal tissue.

MATERIALS AND METHODS

Chemicals. Tris, saponin and 3,3'-diaminobenzidine tetrahydrochloride (DAB) were purchased from Sigma. The rabbit immunohistochemical detection system was from Oncogene Science.

Antibodies. Rabbit anti-ubiquitin and anti-UCRP polyclonal antibodies were generated against SDS-denatured ubiquitin and recombinant mature human UCRP, respectively, and then were affinity purified as described in (13).

Cell Lines and Culture. The primary cell cultures of normal (5757) and AT (1588 and 2052) non-transformed human fibroblasts were obtained from the Coriell Institute (Camden, NJ). Fibroblast cultures were grown in Dulbecco's modified Eagles media (D-MEM, Flow, McLean, VA) supplemented with 10% or 15% heat-inactivated fetal calf serum (FCS, Gibco, Grand Island, NY), penicillin (100 units/ml) and streptomycin (100 μg/ml). All stock cultures were maintained in 75-cm^2 culture flasks at 37°C in incubators with a 5% CO_2/95% air atmosphere.

Immunohistochemistry. Confluent cultures of 5757,1588, and 2052 primary fibroblasts were grown on glass coverslips. The cells were rinsed with phosphate-buffered saline three times and fixed with 80% methanol for at least 20 minutes. Endogenous peroxidase was blocked with 1% H_2O_2 dissolved in 100% methanol for 30 minutes. The coverslips were pre-treated with 0.2% saponin for 30 minutes and the samples were blocked with goat serum for 30 minutes. The coverslips were incubated with anti-ubiquitin (3.2 μg/ml) or anti-UCRP (1 μg/ml) at 4°C overnight. The next day, the cells were incubated for 30 minutes at room temperature with the biotinylated anti-rabbit IgG followed by incubation for 30 minutes with peroxidase-conjugated streptavidin, as specified by the manufacturer. Each step except for the serum block was followed by two rinses in PBS. Diaminobenzidine was used as the

chromogen. The coverslips were counterstained with Gill's haematoxylin, dehydrated and mounted onto slides.

Slides from four individual experiments were coded and scored blindly. The intensity of staining was assessed as negative (0), weak (1), medium (2), or strong (3). The scores for normal and AT cells were averaged for all the experiments and statistical analysis was performed using a standard t-test for two independent samples.

Tissue sections selected for staining were baked overnight on a slide warmer at 37°C and placed in three changes of xylene for 10 minutes each the next day. This was followed by two changes of 100% ethanol lasting 5 minutes each, one change of 95% ethanol for 1 minute, one change of 70% ethanol for 1 minute and, finally, the slides were placed in distilled water. Next, the slides were blocked with 3% H_2O_2 dissolved in 100% methanol for 30 minutes and then, the exact same procedure as described above was followed.

RESULTS

Immunohistochemical Localization of Ubiquitin in Normal and AT Fibroblasts. Two AT fibroblast lines and one normal fibroblast line were grown on glass coverslips to confluency and fixed in 80% methanol. Fixed cells were stained overnight with affinity purified anti-ubiquitin antibody at a concentration of 3.2 μg/ml. The intracellular distribution of ubiquitin was examined using a light microscope where ubiquitin in the cell cytoplasm stained dark brown and the nuclei stained blue. In the normal cell line (Fig.1A), dark brown staining was observed in the cytoplasm suggesting the existence of large ubiquitin pools in stationary phase

normal fibroblasts. In the two AT cell lines (Fig.1B & C), dark brown staining was also observed in the cytoplasm suggesting the existence of large ubiquitin pools in stationary phase AT fibroblasts. Even though this particular experiment was not repeated sufficient times to perform statistical analysis, no apparent difference in staining was observed for ubiquitin between normal and AT cells (See Table 1).

Immunohistochemical Localization of UCRP in Normal and AT Fibroblasts. Two AT fibroblast lines and one normal fibroblast line were grown on glass coverslips to confluency and fixed in 80% methanol. Fixed cells were stained overnight with affinity purified anti-UCRP antibody at a concentration of 1 μg/ml. The intracellular distribution of UCRP was examined as for ubiquitin. In the normal cell line (Fig.2A), little or no cytoplasmic staining was observed, indicating that only a small UCRP pool exists in stationary normal fibroblasts. In the two AT cell lines (Fig.2B & C), dark brown staining was observed with a cytoplasmic fibrous distribution, thereby suggesting the existence of large UCRP pools in stationary AT fibroblasts. UCRP scores were found to be significantly different between normal and AT cells ($P < .025$) [See Table 2]. However, since the UCRP antibody used in the experiments does not distinguish between free and conjugated polypeptide, it was not possible to determine whether the UCRP distribution observed in the AT fibroblasts represents free, conjugated or both forms of UCRP.

Immunohistochemical Localization of UCRP in Normal Tonsil. Normal tonsil tissue was obtained from an individual at surgery, preserved in formaldehyde and embedded in wax. A tissue section was stained overnight with affinity purified anti-UCRP antibody at a concentration of 1 μg/ml. The intracellular distribution of UCRP was examined using a light microscope. In this specimen (Fig.3A), epithelial tissue

from a normal tonsil, very weak cytoplasmic staining was observed around the blue nuclei of the cells suggesting the presence of little UCRP in this normal tissue section. The UCRP levels in these normal epithelial cells are comparable to those in the normal fibroblasts (Fig.2A) suggesting that very low levels of UCRP are normally found in these two types of human cells.

Immunohistochemical Localization of UCRP in Bladder Cancers. Pre-malignant and malignant bladder tissue was obtained from three different adults at surgery, preserved in formaldehyde and embedded in wax. Tissue sections were stained overnight with affinity purified anti-UCRP antibody at a concentration of 1 μg/ml. The intracellular distribution of UCRP was examined using a light microscope. In the first specimen (Fig.3B), a dysplastic lesion of the bladder, some granular cytoplasmic staining was observed in many cells suggesting the accumulation of UCRP in this pre-malignant bladder section. In the second specimen (Fig.3C), an invasive carcinoma of the bladder (grade 3), homogeneous dark brown staining was observed in the cytoplasms of many cells suggesting the existence of large UCRP pools in this tumour section. In the third specimen (Fig.3D), another invasive carcinoma of the bladder (grade 3), homogeneous dark brown cytoplasmic staining was also observed in almost all the cells suggesting the presence of large UCRP pools in this tumour section. Interestingly, as compared with the normal fibroblasts (Fig.2A) and normal epithelial tissue (Fig.3A), the UCRP levels appear to be elevated in the tumour cells and are comparable to the elevation of UCRP observed in the AT fibroblasts. However, as the UCRP antibody used in the experiment does not distinguish between free and conjugated polypeptide, it is not possible to determine whether the UCRP distribution observed in the tumour tissue sections represents free, conjugated or both forms of UCRP.

Immunohistochemical Localization of UCRP in Lung Cancer. Tumour tissue was obtained from an adult with lung cancer at surgery, preserved in formaldehyde and embedded in wax. A tissue section was stained overnight with affinity purified anti-UCRP antibody at a concentration of 1 μg/ml. The intracellular distribution of UCRP was examined using a light microscope. In this lung tumour specimen (Fig.3E), areas of brown cytoplasmic staining were observed around cell nuclei suggesting the existence of UCRP pools in this tumour section. Once again, as compared with the normal fibroblasts (Fig.2A) and normal epithelial tissue (Fig.3A), the UCRP levels appear to be elevated in these tumour cells and are comparable to the elevation of UCRP observed in the AT fibroblasts.

DISCUSSION

From the results obtained using immunochemical techniques, it appears that UCRP levels are constitutively elevated not only in AT cells, which are susceptible to malignant transformation, but also in human tumours including two bladder and one lung cancer specimen. Two different AT fibroblast lines showed extensive cytoplasmic staining with the anti-UCRP antibody, while the corresponding normal fibroblast line had barely detectible levels of UCRP. Sections from a dysplastic lesion of the bladder and two different invasive bladder carcinomas stained highly positive for UCRP. A lung tumour tissue section also stained positively for UCRP, while a normal epithelial tissue section was negative. These results suggest a difference in the dynamics of UCRP pools between AT, pre-malignant and malignant cancer cells, which display high UCRP expression and normal cells, which have low levels of UCRP in comparison. Furthermore, the fact that cells from a pre-malignant bladder lesion

already display elevated UCRP levels suggests that this may be an important step in cells undergoing rapid proliferation or carcinogenesis. The elevation of UCRP in cells from individuals with AT who are highly susceptible to certain cancers further supports this hypothesis.

As the UCRP antibody used in these experiments does not distinguish between free and conjugated polypeptide, it is not possible to determine whether the UCRP distribution observed in the tumour tissue sections represents free, conjugated or both forms of UCRP. However, Western blotting analysis showed that it was free UCRP levels that were elevated in an SV40-transformed normal human fibroblast line as compared to a non-transformed control (unpublished results). Furthermore, previous studies have also shown that the elevated UCRP pools observed in AT fibroblasts represent free UCRP (21). This elevation of UCRP can be blocked by treating the AT cells with neutralizing antibodies against interferon ß over a period of three generations. Thus, constitutive activation of the interferon ß gene causes continuous induction of UCRP in AT cells, probably as a result of a defect in the NF-κB activation pathway. In fact, the gene mutated in ataxia-telangiectasia cells (ATM) has been recently identified as a possible phosphatidylinositol 3-kinase (PI3K) which may be involved in signal transduction (19). An interesting possibility is that the elevation of UCRP observed in the pre-cancer and cancer cells could also result from a similar deregulation of the activation pathway for the interferon ß gene by way of a mutation.

In the past, disturbances in interferon expression have been linked to certain conditions predisposing to cancer. Previously, defective interferon γ production has been reported in peripheral blood mononuclear cells from patients with AT (22). Wasted mice, which spontaneously develop a disease that resembles AT in humans, have also been noted to display abnormalities in interferon production (23). A

reduction in interleukin-6 (IL-6), also known as interferon ß, has been reported in cultured cells from patients with Fanconi's anemia (24). Together, these observations support the importance of normal interferon regulation in maintaining control over cell growth and division.

Tumour suppressor genes are genes that are responsible for inhibiting cell growth by counterbalancing the effects of growth-promoting proto-oncogenes (25). The overexpression of oncogenes caused by a variety of mutational events can result in cellular transformation, while the elimination or inactivation of tumour suppressor genes by mutational events also results in transformation (26). p53 was initially identified as an overexpressed antigen in chemically transformed sarcoma cells suggesting that it was an oncogene. However, wild-type p53 cDNAs were later found to be strongly growth suppressive and to inhibit transformation indicating that it was mutant p53 alleles that favour cell growth (25,27). Thus, like p53, a regulatory component of the interferon ß activation pathway, such as the ATM gene, or the interferon ß gene itself may qualify as a tumour suppressor gene, as any mutation diminishing the normal activity of interferon could have severe consequences for the cell cycle. In this scenario, the elevation of UCRP observed in the cancer cells could be the effect of an event, namely the dysregulation of interferon expression, that occurs early on during tumorigenesis. This could be caused by a mutation in some component of interferon regulation pathway, which could result in decreased inhibitory control over cell division.

In conclusion, AT cells have elevated UCRP levels resulting from constitutive activation of the interferon ß gene. It is likely that the dysregulation of the interferon ß gene in AT cells is caused by the direct effect of the ATM gene product on the interferon ß activation pathway. Since AT cells are predisposed to cancer but are not yet cancer cells, the elevation of UCRP observed in tumour tissue may also

indicate constitutive activation of the interferon ß gene in cancer cells. This could be tested by treating cultured cancer cells with neutralizing antibodies against interferon ß for a period of three generations. If the UCRP elevation in the cancer cells were also found to be caused by constitutive activation of the interferon ß gene, then this would suggest that dysregulation of the interferon ß activation pathway could be directly related to the induction of cancer in cells. Alternatively, interferon ß levels may be elevated in both AT and cancer cells as a response to endogenous carcinogenic stimuli. In either case, the possible clinical application of this research might include using UCRP as a biomarker to identify pre-cancerous and cancerous tissue in its earliest stages of development.

ACKNOWLEDGEMENTS

We would like to thank Dr. Ann Worth, M.D. (Pathologist, British Columbia Cancer Control Agency) whose extensive knowledge of cancer pathology significantly contributed to the interpretation of the data presented in this paper. We would also like to thank Ms. Carmen Michelsen for her technical assistance with the immunohistochemistry.

REFERENCES

1. Hershko, A. and Ciechanover, A. The ubiquitin system for protein degradation. Ann. Rev. Biochem., 61: 761-807, 1992.
2. Goldberg, A.L. and Rock, K.L. Proteolysis, proteasomes and antigen presentation. Nature, 357: 375-379, 1992.
3. Tanaka, K., Tamura, T., Yoshimura, T. and Ichihara, A. Proteasomes: protein and gene structures. New Biol., 4(3): 173-187, 1992.
4. Jentsch, S., McGrath, J.P., and Varshavsky, A. The yeast DNA repair gene RAD6 encodes a ubiquitin-conjugating enzyme. Nature, 329: 131-134, 1987.
5. Goebl, M.G., Yochem, J., Jentsch, S., McGrath, J.P., Varshavsky, A., and Byers, B. The yeast cell cycle gene CDC34 encodes a ubiquitin-conjugating enzyme. Science, 241: 1331-1335, 1988.
6. John, T.S., Gallatin, W.M., Siegelman, M., Smith, H.T., Fried, V.A., and Weissman, I.L. Expreesion cloning of a lymphocyte homing receptor cDNA: ubiquitin is the reactive species. Science, 231: 845-850, 1986.
7. Finley, D., Bartel, B., and Varshavsky, A. The tails of ubiquitin precursors are ribosomal proteins whose fusion to ubiquitin facilitates ribosome biogenesis. Nature, 338: 394-401, 1989.
8. Ciechanover, A., DiGiuseppe, J.A., Bercovich, B., Orian, A., Richter, J.D., Schwartz, A.L., and Brodeur, G.M. Degradation of nuclear oncoproteins by the ubiquitin system in vitro. Proc. Natl. Acad. Sci. USA, 88: 139-143, 1991.
9. Scheffner, M., Huibregtse, J.M., and Howley, P.M. Identification of a human ubiquitin-conjugating enzyme that mediates the E6-AP-dependent ubiquitination of p53. Proc. Natl. Acad. Sci. USA, 91: 8797-8801, 1994.

10. Pines, J. Ubiquitin with everything. Nature, 371: 742-743, 1994.

11. Kanayama, H., Tanaka, K., Aki, M., Kagawa, S., Miyaji, H., Satoh, M., Okada,F., Sato, S., Shimbara, N. and Ichihara, A. Changes in expressions of proteasome and ubiquitin genes in human renal cancer cells. Cancer Res., 51: 667-6685, 1991.

12. Kumatori, A., Tanaka, K., Inamura, N., Sone, S., Ogura, T., Matsumoto, T., Tachikawa, T., Shin, S. and Ichihara, A. Abnormally high expression of proteasomes in human leukemic cells. Proc. Natl. Acad. Sci. USA, 87: 7071-7075, 1990.

13. Haas, A.L., Ahrens, P., Bright, P.M., and Ankel, H. Interferon induces a 15-kilodalton protein exhibiting marked homology to ubiquitin. J. Biol. Chem., 262 (23): 11315-11323, 1987.

14. Sen, G.C. and Lengyel, P. The interferon system. J. Biol. Chem., 267(8):5017-5020, 1992.

15. Levy, N., Yonish-Rouach, E., Oren, M. and Kimchi, A. Complementation by wild-type p53 of interleukin-6 effects on M1 cells: induction of cell cycle exit and cooperativity with c-myc suppression. Mol. & Cell. Biol., 13(12): 7942-7952, 1993.

16. Loeb, K.R. and Haas, A.L. The interferon-inducible 15-kDa ubiquitin homolog conjugates to intracellular proteins. J. Biol. Chem., 267(11): 7806-7813, 1992.

17. Loeb, K.R. and Haas, A.L. Cytoskeletal distribution of UCRP conjugates. Mol. & Cell. Biol., 14(12): 8408-8419, 1994.

18. Andreassen, P.R. and Margolis, R.L. Microtubule dependency of $p34^{cdc2}$ inactivation and mitotic exit in mammalian cells. J. Cell. Biol., 127 (3): 789-802, 1994.

19. Savitsky, K., Bar-Shira, A., Shlomit, G., Rotman, G., Ziv, Y., Vanagaite, L., Tagle, D.A., Smith, S., Uziel, T., Sfez, S., Askenazi, M., Pecker, I., Frydman, M., Harnik, R., Patanjali, S.R., Simmons, A., Clines, G.A., Sartiel, A., Gatti, R.A., Chessa, L., Sanal, O., Lavin, M.F., Jaspers, N.G.J., Taylor, M.R., Arlett, C.F., Miki, T., Weissman, S.W Lovett, M., Collins, F.S. and Shiloh, Y. A single ataxia telangiectasia gene with a product similar to PI-3 kinase. Science, 268: 1749-1753, 1995.

20. Young, B.R., and Painter, R.B. Radioresistant DNA synthesis and human genetic diseases. Hum. Genet., 82: 113-117, 1989.

21. Siddoo-Atwal, C., Haas, A.L., and Rosin, M.P. Elevation of interferon ß-inducible proteins in ataxia telangiectasia cells. Cancer Res., 56: 443-447, 1996.

22. Paganelli, R., Capobianchi, M.R., Matricardi, P.M., Cioe, L., Seminara,R., Dianzani, F., and Aiuti, F. Defective interferon-γ production in ataxia-telangiectasia. Clin. Immunol. & Immunopathol., 32: 387-391, 1984.

23. Libertin, C.R., Ling-Indeck, L., Padilla, M., and Woloschak, G.E. Cytokine and T-cell subset abnormalities in immunodeficient wasted mice. Mol. Immunol., 31(10): 753-759, 1994.

24. Roselli, F., Sanceau, J., Wietzerbin, J., and Moustacchi, E. Abnormal lymphokine production: a novel feature of the genetic disease Fanconi anemia. Hum. Genet., 89: 42-48, 1992.

25. Weinberg, R.A. Tumour suppressor genes. Science, 254: 1138-1145, 1991

26. Solomon, E., Borrow, J., and Goddard, A.D. Chromosome aberrations and cancer. Science, 254: 1153-1160, 1991.

27. Selter, H. and Montenarh, M. The emerging picture of p53. Int. J. Biochem., 26 (2): 145-154, 1994.

FIGURE LEGENDS

Figure 1. Immunohistochemical Detection of Ubiquitin in Normal and AT Fibroblasts. Normal (5757) and AT (1588,2052) fibroblast cultures were grown on glass coverslips to confluency, rinsed with PBS three times and fixed in 80% methanol. The fixed cells were treated with anti-ubiquitin (3.2 μg/ml) in blocking solution followed by incubation with a biotynylated secondary antibody and then with peroxidase-conjugated streptavidin. **A.** normal (5757) fibroblasts **B.** AT (1588) fibroblasts **C.** AT (2052) fibroblasts

Figure 2. Immunohistochemical Detection of UCRP in Normal and AT Fibroblasts. Normal (5757) and AT (1588,2052) fibroblast cultures were grown on glass coverslips to confluency, rinsed with PBS three times and fixed in 80% methanol. The fixed cells were treated with anti-UCRP (1 μg/ml) in blocking solution followed by incubation with a biotynylated secondary antibody and then with peroxidase-conjugated streptavidin. **A.** normal (5757) fibroblasts **B.** AT (1588) fibroblasts **C.** AT (2052) fibroblasts

Figure 3. Immunohistochemical Detection of UCRP in Normal, Dysplastic and Neoplastic Tissues. Normal, dysplastic, and cancer tissue sections were treated with anti-UCRP (1 μg/ml) in blocking solution followed by incubation with a biotynylated secondary antibody and then with peroxidase-conjugated streptavidin. **A.** normal tonsil **B.** dysplastic bladder **C.** bladder tumour **D.** bladder tumour **E.** lung tumour

Figure 1.

A.

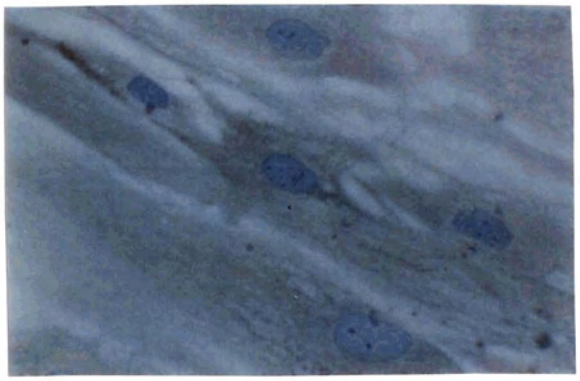

B.

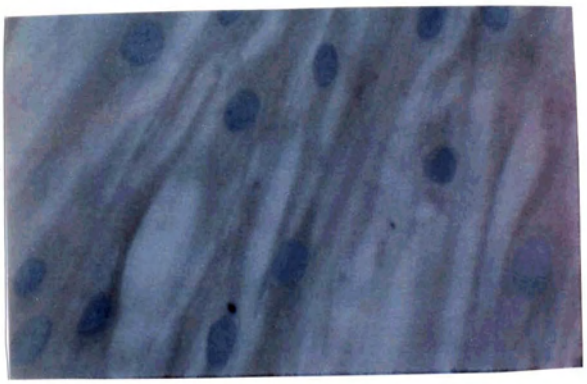

C.

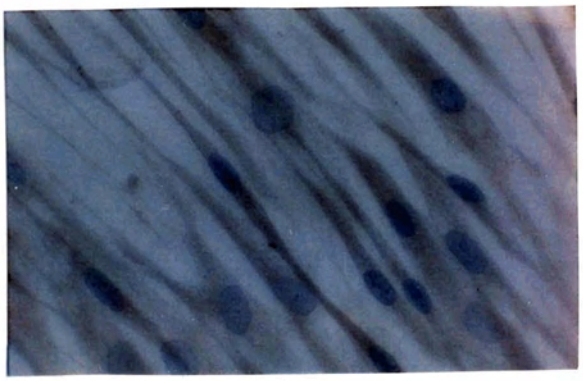

Figure 2.

A.

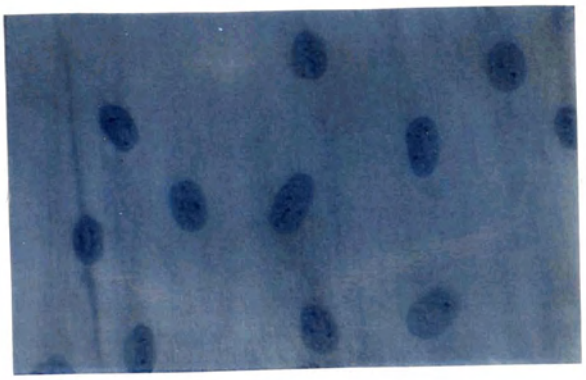

B.

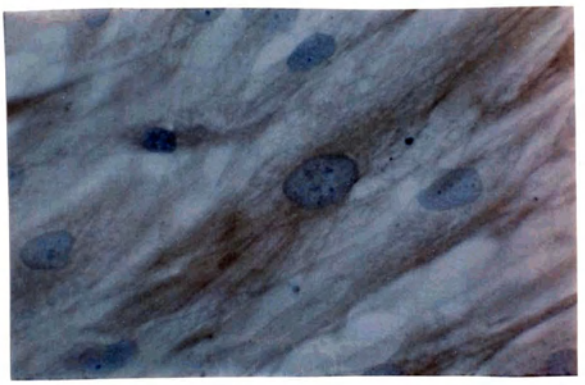

C.

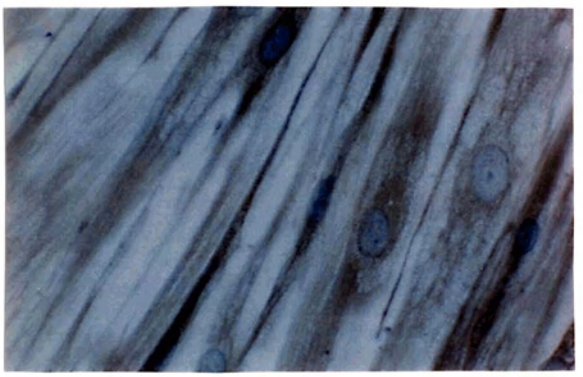

Figure 3.

A.

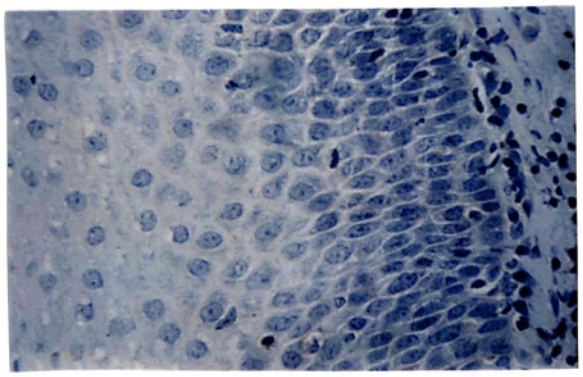

B.

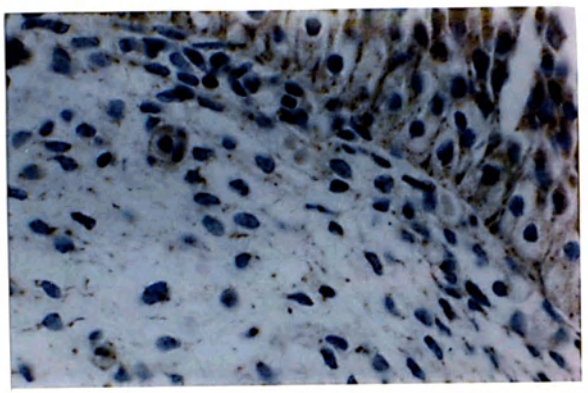

C.

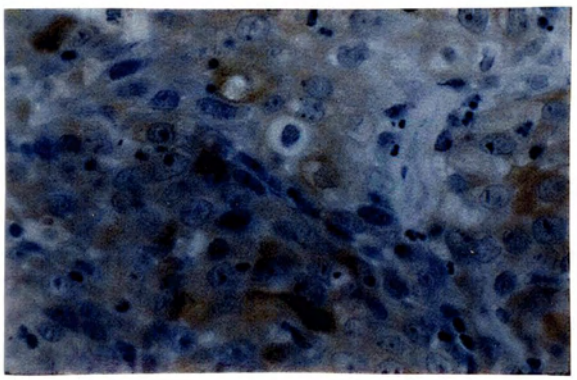

D.

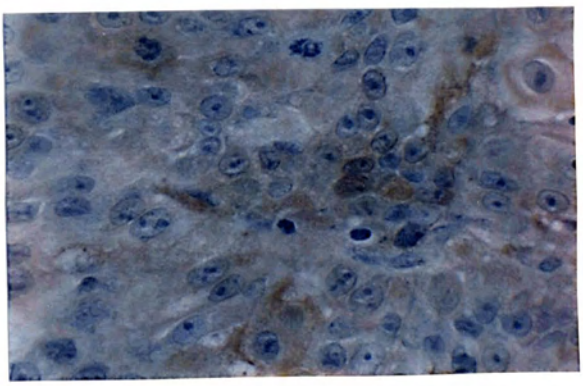

E.

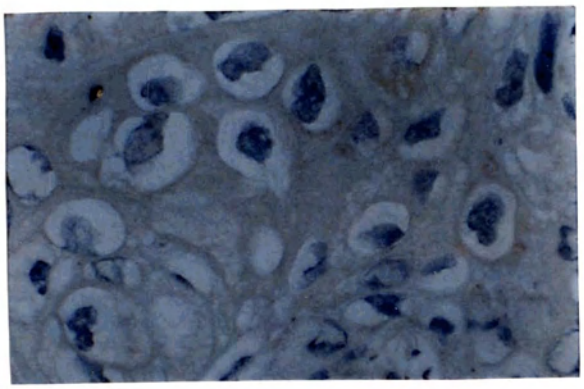

Table 1. Ubiquitin Immunoreactivity in Normal and AT Fibroblasts †					
Number of cells showing indicated level of immunoreactivity (/500)‡					
		0	1	2	3
Normal	5757	0	0	4	496
AT	1588	0	0	0	500
	2052	0	0	10	490

† Results of one experiment.
‡ Intensity was assessed as negative (0), weak (1), medium (2), or strong (3) and 500 cells were scored per slide. Controls in which antibody was omitted showed 0 staining.

Table 2. UCRP Immunoreactivity Normal and AT Fibroblasts †					
Number of cells showing indicated level of immunoreactivity (/500)‡					
		0	1	2	3
Normal	5757	0	500	0	0
		0	498	2	0
		309	191	0	0
		111	389	0	0
AT	1588	0	0	44	456
		0	0	26	474
		0	0	222	278
		0	0	210	290
	2052	0	0	65	435
		0	0	73	427
		0	0	9	491
		0	0	257	243

† Results of four separate experiments.
‡ Intensity was assessed as negative (0), weak (1), medium (2), or strong (3) and 500 cells were scored per slide. Controls in which antibody was omitted showed 0 staining.
• Significance was $P < .025$ comparing the means of N (5757) and AT (1588).
• Significance was $P < .025$ comparing the means of N (5757) and AT (2052).

CONCLUSION

Studies of the cellular defect resulting in the AT phenotype have identified several features which suggest a defect in a central DNA damage response pathway involving a G1 growth-arrest mechanism such as defective induction of stress-activated protein (SAP) kinase activity and p53 following X-irradiation, constitutive activation of NF-κB, and constitutive activation of the interferon ß gene (as part of this thesis) [42,47,48]. The AT gene product is a relative of DNA-dependent protein kinase, which is a relative of PI 3-kinase. If the ATM protein is a DNA-PK-like protein, then it would be expected to affect Jun, Fos, Myc and p53 regulation and, therefore, to have an impact on the G1 checkpoint. In support of this hypothesis, faulty p53 induction in response to ionizing radiation treatment has been correlated with the absence of a G1 arrest in AT cells [47]. Furthermore, recent evidence indicates that PI 3-kinase activity may be normally important in regulating the p53-dependent G1 checkpoint in response to X-ray-induced DNA damage [54]. p53 has also been reported to produce a coordinate growth arrest in M1 cells with interferon ß suggesting that interferon ß may cooperate with p53 in preventing efficient entry into S phase [46]. Tumour necrosis factor-α, one of the inducers of interferon ß, can activate NF-κB which, in turn, has been shown to stimulate p53 activation [49]. IRF (interferon regulatory factor) binding to upstream IRF sequences in the p53 promoter has also been reported [50]. Together with the above observations, the anti-proliferative properties of interferon ß would be consistent with its possible participation in a G1 growth-arrest mechanism in response to DNA damage. If this is the case, altered activation of NF-κB, IRF, or Jun by a mutant AT protein could affect activation of the interferon ß gene and result in altered interferon ß regulation in response to DNA damage.

AT cells are more susceptible to cancer: how could the constitutive activation of the interferon ß gene be linked to carcinogenesis? A possible mechanism would be that the ATM protein, a PI 3-kinase, constitutively activates a signal transduction pathway resulting in the downstream constitutive activation of the interferon ß gene. The level of interferon ß induced in AT cells is sufficient to decrease cell growth rate but is not enough to arrest cell division. At the same time, the mutant kinase is not responsive to its usual activators which normally induce a state of cell cycle arrest in dividing cells by increasing interferon ß and p53 levels. Thus, this DNA damage response pathway including G1 arrest does not operate in AT cells following exposure to stimuli such as X-irradiation and, therefore, the cells cannot repair the resulting DNA damage. Instead, the AT cells continue to divide slowly, thereby replicating mutations caused by the DNA damaging agent; the accumulation of these mutations ultimately results in cancer (See Figure 5).

The data presented in this thesis are consistent with the above hypothesis that the interferon ß gene may not only be activated in response to viral infection but may also play an important role in growth arrest following DNA damage. Firstly, these studies have shown that the activation pathway for the interferon ß gene is dysregulated in AT cells which may have a faulty DNA damage response pathway. Secondly, the elevation of UCRP is an indirect indication of the altered interferon ß regulation in both AT and cancer cells, thereby suggesting a role for interferon ß in maintaining normal cell growth and division. So far, studies have not been performed to rule out this possibility. However, further experimental evidence for direct involvement of interferon ß in the G1 growth-arrest mechanism is required. To accomplish this, one could treat synchronized cells in G1 phase of the cell cycle with X-rays and testing for the subsequent induction of interferon ß or UCRP by flow cytometry and/or immunoblotting analysis. Induction of this DNA damage

response pathway would be expected to be defective in AT cells following exposure to X-rays.

Finally, it is interesting to consider the possible consequences of elevated levels of interferon ß and interferon ß-inducible proteins, such as UCRP and LMP2, in AT cells. The biochemical function of UCRP conjugation to proteins awaits elucidation. However, UCRP has been recently found to act extracellularly as a cytokine in the subsequent induction of interferon γ in human cells [51]. The role of interferon γ in cells is primarily as an immunoregulator [37]. One of its effects is to induce the synthesis of LMP2 and LMP7 proteasomal subunits resulting in altered proteasome composition and, therefore, in proteolytic specificity [25]. Proteasomes have been shown to perform at least two essential cellular functions: firstly, catalyzing antigen processing and, secondly, regulating the cell cycle by specific proteolysis [29]. Changes in proteasome composition may effect both of these activities [24,52]. Interestingly, AT patients characteristically display certain immunological defects and a propensity for developing cancer, particularly lymphoreticular malignancies. Just recently, interferon γ treatment of vascular cells has been shown to indirectly induce apoptosis in human leukemic cells [60]. Thus, it is possible that the elevation of interferon ß and certain interferon ß-inducible proteins observed in cultured cells from AT patients may be associated with some of the clinical manifestations of this disease.

Figure 5. Hypothetical Pathway for G1 Growth-Arrest

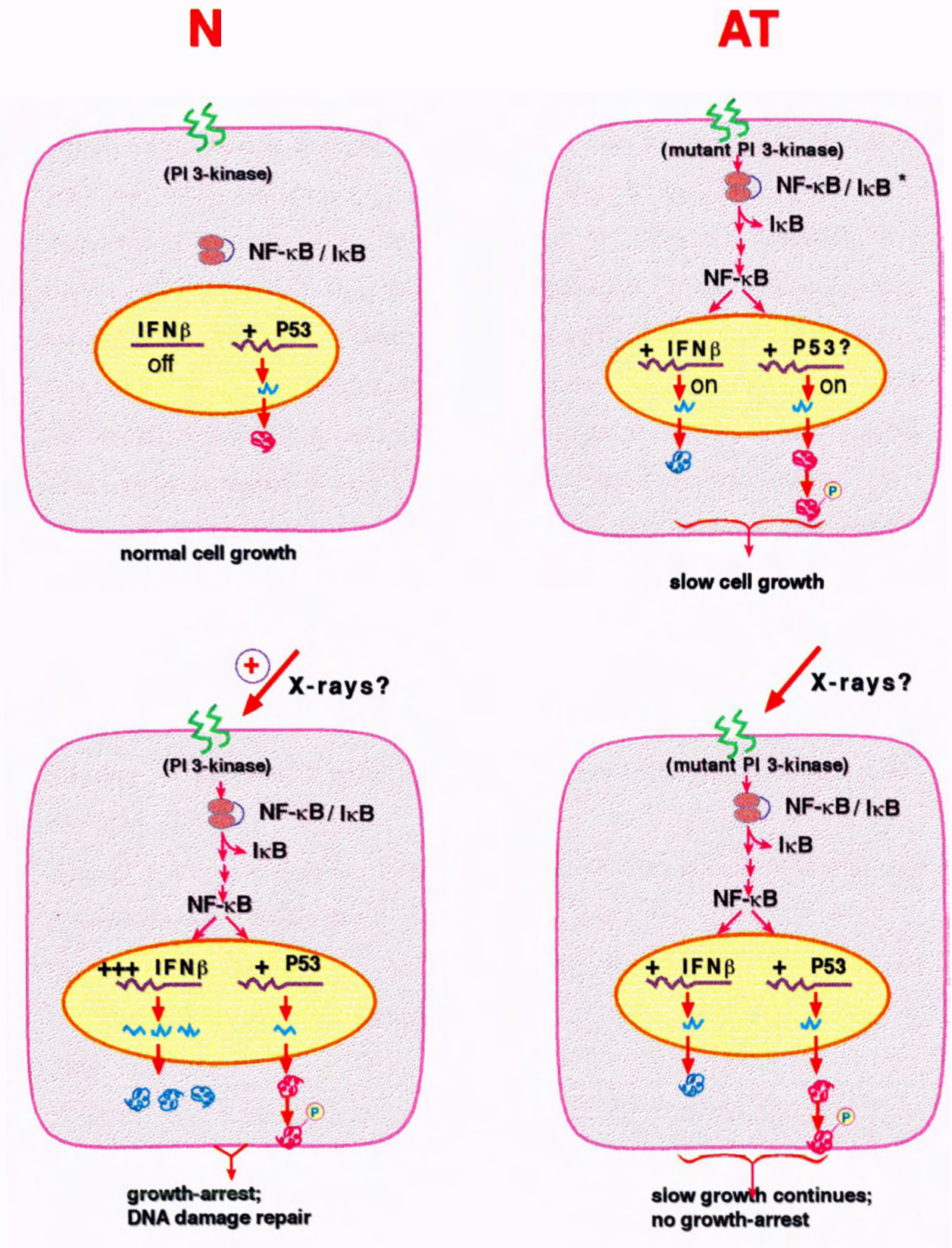

* modified IkB transcript that does not inhibit NF-κB effectively

REFERENCES

1. Boder, E. Ataxia-telangiectasia: An overview. In: Gatti, R., Swift, M., eds. Ataxia-Telangiectasia: Genetics, Neuropathology, and Immunology of a Degenerative Disease of Childhood. New York: Alan R. Liss, pp 1-63, 1985.
2. Savitsky, K., Bar-Shira, A., Shlomit, G., Rotman, G., Ziv, Y., Vanagaite, L., Tagle, D.A., Smith, S., Uziel, T., Sfez, S., Askenazi, M., Pecker, I., Frydman, M., Harnik, R., Patanjali, S.R., Simmons, A., Clines, G.A., Sartiel, A., Gatti, R.A., Chessa, L., Sanal, O., Lavin, M.F., Jaspers, N.G.J., Taylor, M.R., Arlett, C.F., Miki, T., Weissman, S.W Lovett, M., Collins, F.S. and Shiloh, Y. A single ataxia telangiectasia gene with a product similar to PI-3 kinase. Science, 268: 1749-1753, 1995.
3. McKinnon, P.J. Ataxia-telangiectasia: an inherited disorder of ionizing-radiation sensitivity in man. Hum. Genet., 75: 197-208, 1987.
4. Gatti, R.A., Boder, E., Vinters, H.V., Sparkes, R.S., Norman, A., and Lange, K. Ataxia-Telangiectasia: an interdisciplinary approach to pathogenesis. Medicine, 70 (2): 99-117, 1991.
5. Thacker, J. Inherited sensitivity to x-rays in man. Bioessays, 11 (2&3): 58-62, 1989.
6. Young, B.R., and Painter, R.B. Radioresistant DNA synthesis and human genetic diseases. Hum. Genet., 82: 113-117, 1989.
7. Taylor, A.M.R., Byrd, P.J., McConville, C.M., and Thacker, S. Genetic and cellular features of ataxia telangiectasia. Int. J. Radiat. Biol., 65 (1): 65-70, 1994.
8. Beamish, H., Khanna, K., Lavin, M.F., Ionizing radiation and cell cycle progression in ataxia telangiectasia. Radiat. Res., 138: S130-S133, 1994.

9. Beamish, H., and Lavin, M.F., Radiosensitivity in ataxia telangiectasia: anomalies in radiation-induced cell cycle delay. Int. J. Radiat. Biol., 65(2): 175-184, 1994.

10. Gatti, R.A. Localizing the genes for ataxia-telangiectasia: a human model for inherited cancer susceptibility. Adv. Cancer Res., 56: 77-104, 1991.

11. Ambrose, H.J., Byrd, P.J., McConville, C.M., Cooper, P.R., Stankovic, T., Riley, J.H., Shiloh, Y., McNamara, J.O., Fukao, T., and Taylor, A.M.R. A physical map across chromosome 11q22-q23 containing the major locus for ataxia-telangiectasia. Genomics, 21: 612-619, 1994.

12. Kastan, M. Ataxia-telangiectasia - broad implications for a rare disorder. New Engl. J. Med., 333 (10): 662-663, 1995.

13. Solomon, E., Borrow, J., Goddard, A.D. Chromosome aberrations and cancer. Science, 254: 1153-1160, 1991.

14. Norbury, C, and Nurse, P. Animal cell cycles and their control. Ann. Rev. Biochem., 61: 441-70, 1992.

15. Murray, A.W. Creative blocks: cell-cycle checkpoints and feedback controls. Nature, 359: 599-604, 1992.

16. Hunter, T. and Pines, J. Cyclins and cancer II: cyclin D and CDK inhibitors come of age. Cell, 79: 573-582, 1994.

17. Hershko, A. and Ciechanover, A. The ubiquitin system for protein degradation. Ann. Rev. Biochem., 61: 761-807, 1992.

18. Glotzer, M., Murray, A.W., and Kirschner, M.W. Cyclin is degraded by the ubiquitin pathway. Nature, 349: 132-138, 1991.

19. Motokura, T., Keyomarsi, K., Kronenberg, H.M., and Arnold, A. Cloning and characterization of human cyclin D3, a cDNA closely related in sequence to the PRAD1/cyclin D1 proto-oncogene. J. Biol. Chem., 267 (28): 20412-20415, 1992.

20. Goldberg, A.L. and Rock, K.L. Proteolysis, proteasomes and antigen presentation. Nature, 357: 375-379, 1992.

21. Tanaka, K., Tamura, T., Yoshimura, T. and Ichihara, A. Proteasomes: protein and gene structures. New Biol., 4(3): 173-187, 1992.

22. Mayer, R.J. and Doherty, F.J. Ubiquitin. Essays - Biochem., 27: 37-48, 1992.

23. Fischer, M., Hilt, W., Richter-Ruoff, B., Gonen, H., Ciechanover, A., and Wolf, D.H. The 26S proteasome of the yeast Saccharomyces cerevisiae. FEBS Lett., 355: 69-75, 1994.

24. Tanaka, K. Molecular biology of proteasomes. Mol. Biol. Reports, 21: 21-26, 1995.

25. Aki, M., Shimbara, N., Takashina, M., Akiyama, K., Kagawa, S., Tamura, T., Tanahashi, N., Yoshimura, T., Tanaka, K. and Ichihara, A. Interferon γ induces different subunit organizations and functional diversity of proteasomes. J. Biochem., 115: 257-269, 1994.

26. Scheffner, M., Huibregtse, J.M., and Howley, P.M. Identification of a human ubiquitin-conjugating enzyme that mediates the E6-AP-dependent ubiquitination of p53. Proc. Natl. Acad. Sci. USA, 91: 8797-8801, 1994.

27. Ciechanover, A., DiGiuseppe, J.A., Bercovich, B., Orian, A., Richter, J.D., Schwartz, A.L., and Brodeur, G.M. Degradation of nuclear oncoproteins by the ubiquitin system in vitro. Proc. Natl. Acad. Sci. USA, 88: 139-143, 1991.

28. Palombella, V.J., Rando, O.J., Goldberg, A.L., and Maniatis, T. The ubiquitin-proteasome pathway is required for processing the NF-κB1 precursor protein and the activation of NF-κB. Cell, 78: 773-785, 1994.

29. Ichihara, A. and Tanaka, K. Roles of proteasomes in cell growth. Mol. Biol. Reports, 21: 49-52, 1995.

30. Jentsch, S., McGrath, J.P., and Varshavsky, A. The yeast DNA repair gene RAD6 encodes a ubiquitin-conjugating enzyme. Nature, 329: 131-134, 1987.

31. Goebl, M.G., Yochem, J., Jentsch, S., McGrath, J.P., Varshavsky, A., and Byers, B. The yeast cell cycle gene CDC34 encodes a ubiquitin-conjugating enzyme. Science, 241: 1331-1335, 1988.

32. Weinert, T.A. and Hartwell, L.H. The RAD9 gene controls the cell cycle response to DNA damage in Saccharomyces cerevisiae. Science, 241: 317-322, 1988.

33. Hodgins, R.R., Ellison, K.S., and Ellison, M.J. Expression of a ubiquitin derivative that conjugates to protein irreversibly produces phenotypes consistent with a ubiquitin deficiency. J. Biol. Chem., 267 (13): 8807-8812, 1992.

34. Knight, E. and Cordova, B. IFN-induced 15-kDa protein is released from human lymphocytes and monocytes. J. Immunol., 146: 2280-2284, 1991.

35. Haas, A.L., Ahrens, P., Bright, P.M., and Ankel, H. Interferon induces a 15-kilodalton protein exhibiting marked homology to ubiquitin. J. Biol. Chem., 262 (23): 11315-11323, 1987.

36. Loeb, K.R. and Haas, A.L. The interferon-inducible 15-kDa ubiquitin homolog conjugates to intracellular proteins. J. Biol. Chem., 267(11): 7806-7813, 1992.

37. Sen, G.C. and Lengyel, P. The interferon system. J. Biol. Chem., 267(8):5017-5020, 1992.

38. Loeb, K.R. and Haas, A.L. Cytoskeletal distribution of UCRP conjugates. Mol. & Cell. Biol., 14(12): 8408-8419, 1994.

39. Keith, C.T. and Schreiber, S.L. PIK-related kinases: DNA repair, recombination, and cell cycle checkpoints. Science, 270: 50-51, 1995.

40. Hartley, K.O., Gell, D., Smith, G.C.M., Zhang, H., Divecha, N., Connelly, M.A., Admon, A., Lees-Miller, S.P., Anderson, C.W., and Jackson, S.P. DNA-dependent protein kinase catalytic subunit: a relative of phosphatidylinositol 3-kinase and the ataxia telangiectasia gene product. Cell, 82: 849-856, 1995.

41. Anderson, C.W. DNA damage and the DNA-activated protein kinase. TIBS, 18: 433-437, 1993.

42. Shafman, T.D., Saleem, A., Kyriakis, J., Weichselbaum, R., Kharbanda,S., and Kufe, D.W. Defective induction of stress-activated protein kinase activity in ataxia-telangiectasia cells exposed to ionizing radiation. Cancer Res., 55: 3242-3245, 1995.

43. Baeuerle, P.A. and Henkel, T. Function and activation of NF-κB in the immune system. Ann. Rev. Immunol., 12: 141-179, 1994

44. Thanos, D. and Maniatis, T. NF-κB: A lesson in family values. Cell, 80: 529-532, 1995.

45. Du, W., Thanos, D., and Maniatis, T. Mechanisms of transcriptional synergism between distinct virus-inducible enhancer elements. Cell, 74: 887-898, 1993.

46. Levy, N., Yonish-Rouach, E., Oren, M. and Kimchi, A. Complementation by wild-type p53 of interleukin-6 effects on M1 cells: induction of cell cycle exit and cooperativity with c-myc suppression. Mol. & Cell. Biol., 13(12): 7942-7952, 1993.

47. Kastan, M.B., Zhan, Q., El-Deiry, W., Carrier, F., Jacks, T., Walsh, W.V., Plunkett, B.S., Vogelstein, B., and Fornace, A.J. A mammalian cell cycle

checkpoint pathway utilizing p53 and GADD45 is defective in ataxia-telangiectasia. Cell, 71: 587-597, 1992.

48. Jung, M., Zhang, Y., Lee, S. and Dritschilo, A. Correction of radiation sensitivity in ataxia-telangiectasia cells by a truncated IκB-α. Science, 268: 1619-1621, 1995.

49. Wu, H. and Lozano, G. NF-κB activates p53 in response to stress. J. Biol. Chem., 269: 20067-20074, 1994.

50. Tanaka, N., Kawakami, T., and Taniguchi, T. Recognition DNA sequences of interferon regulatory factor 1 (IRF-1) and IRF-2, regulators of cell growth and the interferon system. Mol. & Cell. Biol., 13 (8): 4531-4538, 1993.

51. D'Cunha, J., Knight, E., Haas, A.L., Truitt, R.L., and Haas, A.L. Immunoregulatory properties of ISG15, an interferon-induced cytokine. Proc. Natl. Acad. Sci. USA, 93: 211-215, 1996.

52. Tanaka, K. Role of proteasomes modified by interferon-γ in antigen processing. J. Leuk. Biol., 56 (5): 571-575, 1994.

53. Riley, D.A., Bain, J.L.W., Ellis, S., and Haas, A.L. Quantitation and immunocytochemical localization of ubiquitin conjugates within red rat and white skeletal muscles. J. Hist. & Cyt., 36(6): 621-632, 1988.

54. Price, B.D. and Youmell, M.B. The phosphatidylinositol 3-kinase inhibitor wortmannin sensitizes murine fibroblasts and human tumour cells to radiation and blocks induction of p53 following DNA damage. Cancer Res., 56: 246-250, 1996.

55. Kapeller, R. and Cantley, L.C. Phosphatidylinositol 3-kinase. Bioessays, 16(8): 565-576, 1994.

56. Meyn, S.M. Ataxia-telangiectasia and cellular responses to DNA damage. Cancer Res., 55: 5991-6001, 1995.

57. Meyn, S.M., Strasfeld, L., and Allen, C. Testing the role of p53 in the expression of genetic instability and apoptosis in ataxia-telangiectasia. Int. J. Radiat. Biol., 66(6): S141-S149, 1994.

58. Duchaud, E., Ridet, A., Stoppa-Lyonnet, D., Janin, N., Moustacchi, E., and Roselli, F. Deregulated apoptosis in ataxia telangiectasia: association with clinical stigmata and radiosensitivity. Cancer Res., 56: 1400-1404, 1996.

59. Brzoska, P.M., Chen, H., Zhu, Y, Levin, N.A., Disatnik, M., Mochly-Rosen, D., Murnane, J.P., and Christman, M.F. The product of the ataxia-telangiectasia group D complementing gene, ATDC, interacts with a protein kinase C substrate and inhibitor. Proc. Natl. Acad. Sci. USA, 92: 7824-7828, 1995.

60. Geng, Y., Hellstrand, K., Wennmalm, A., and Hansson, G.K. Apoptotic death of human leukemic cells induced by vascular cells expressing nitric oxide synthase in response to γ-interferon and tumour necrosis factor-α. Cancer Res., 56: 866-874, 1996.